

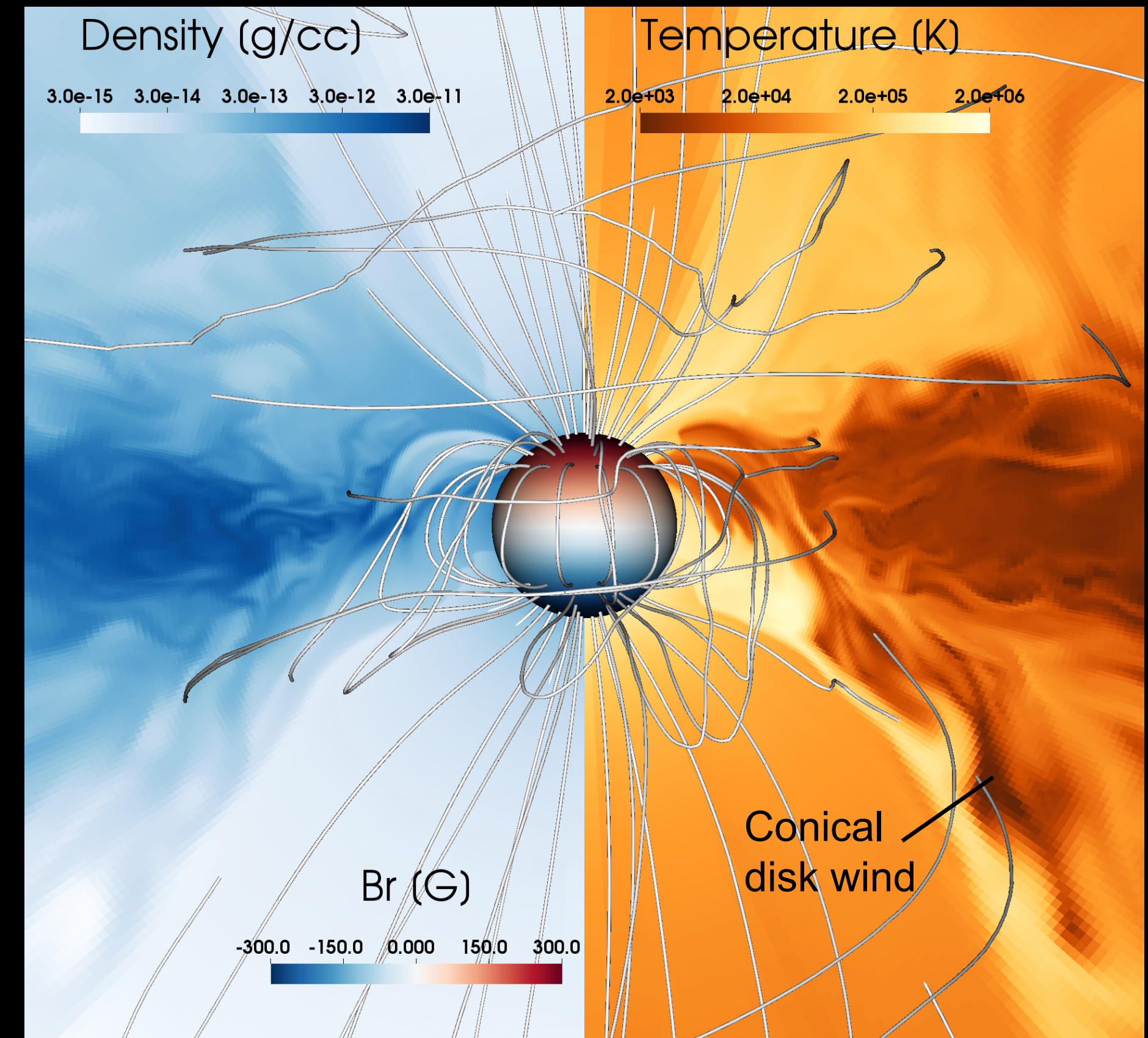
3D MHD simulations of star-disk interaction

Shinsuke Takasao (Osaka Univ., Japan)

Collaborators:

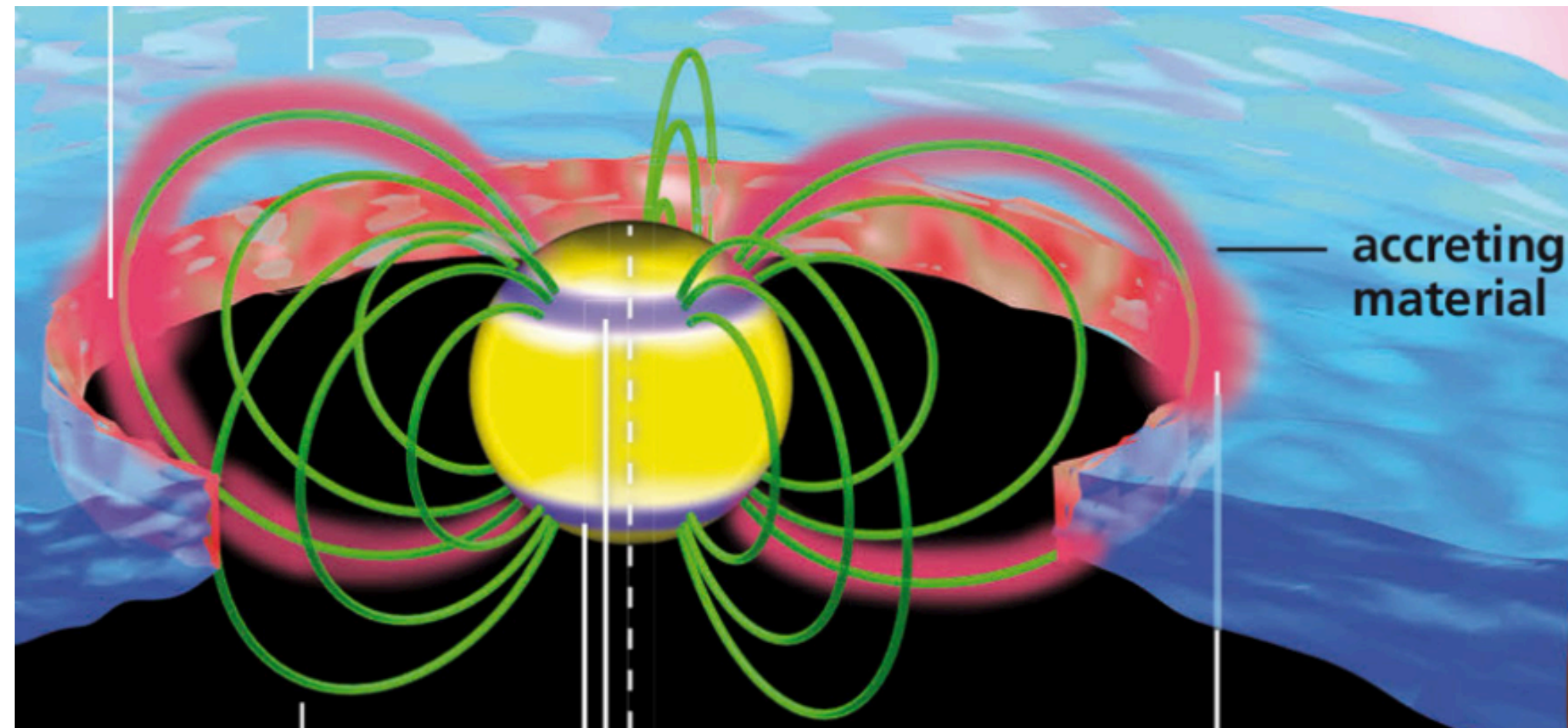
K. Tomida (Tohoku U), K. Iwasaki (NAOJ), T. K. Suzuki (U Tokyo)

Ref. Takasao et al. 2022 ApJ



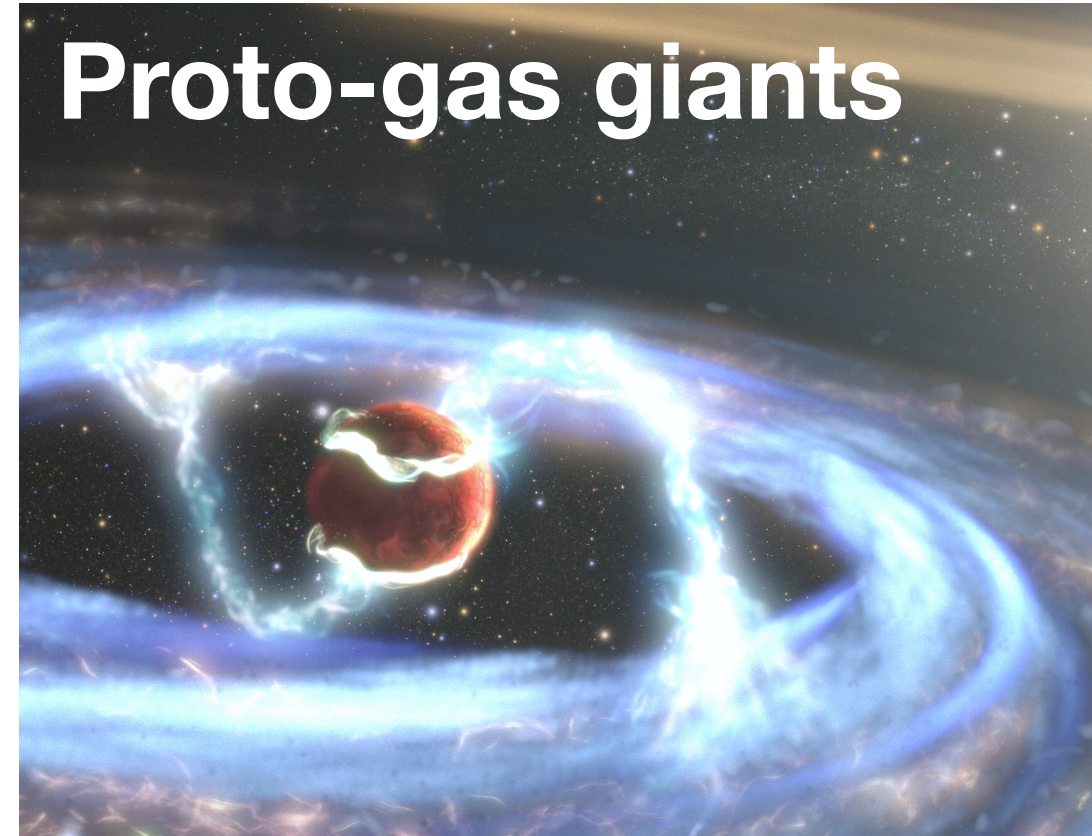
Magnetospheric accretion

T Tauri stars (pre-main-seq. stars)

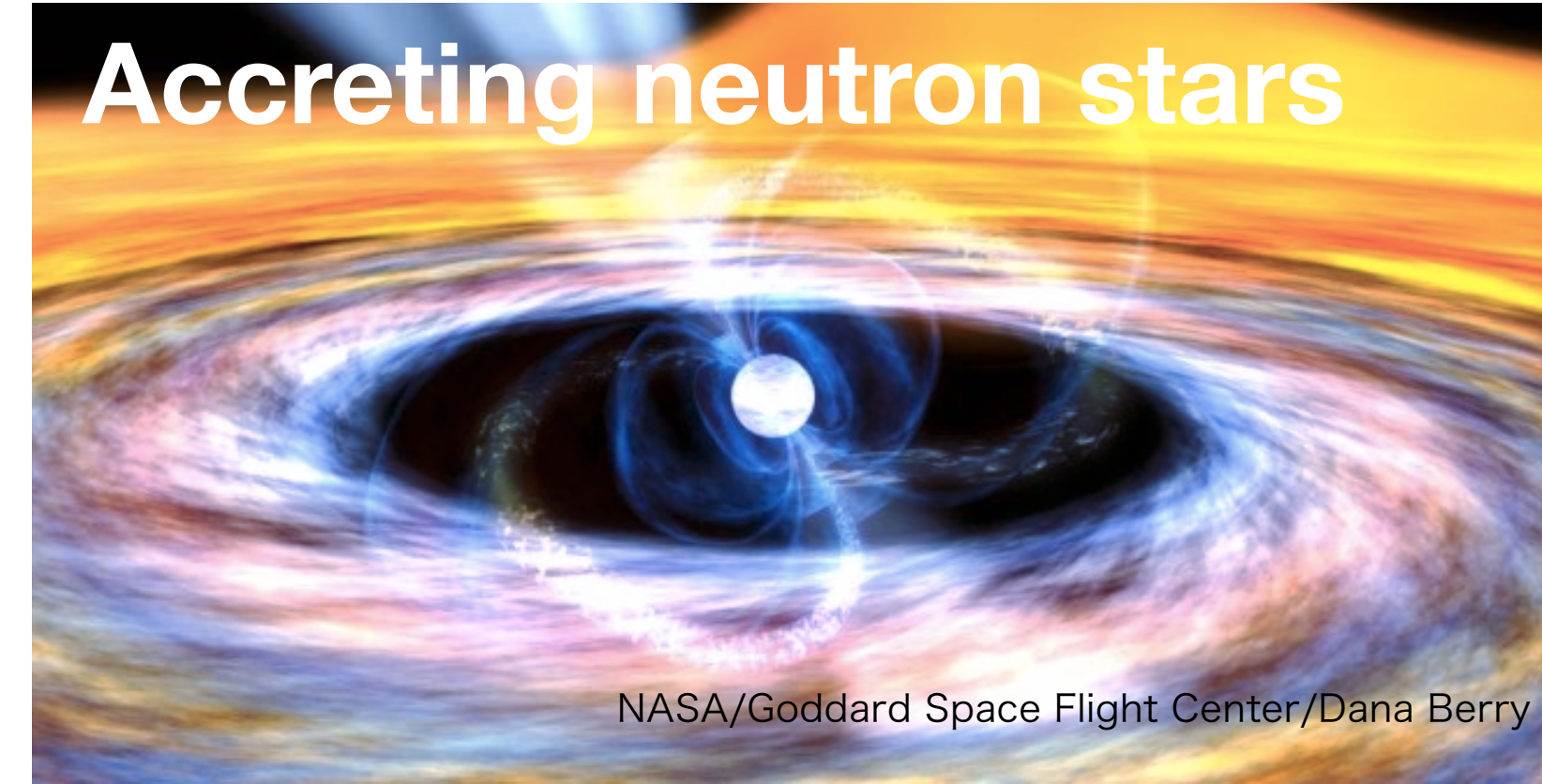


Schematic picture of TW Hya (GRAVITY collaboration 2021)

Proto-gas giants



Accreting neutron stars



NASA/Goddard Space Flight Center/Dana Berry

General accretion mode in strongly magnetized objects

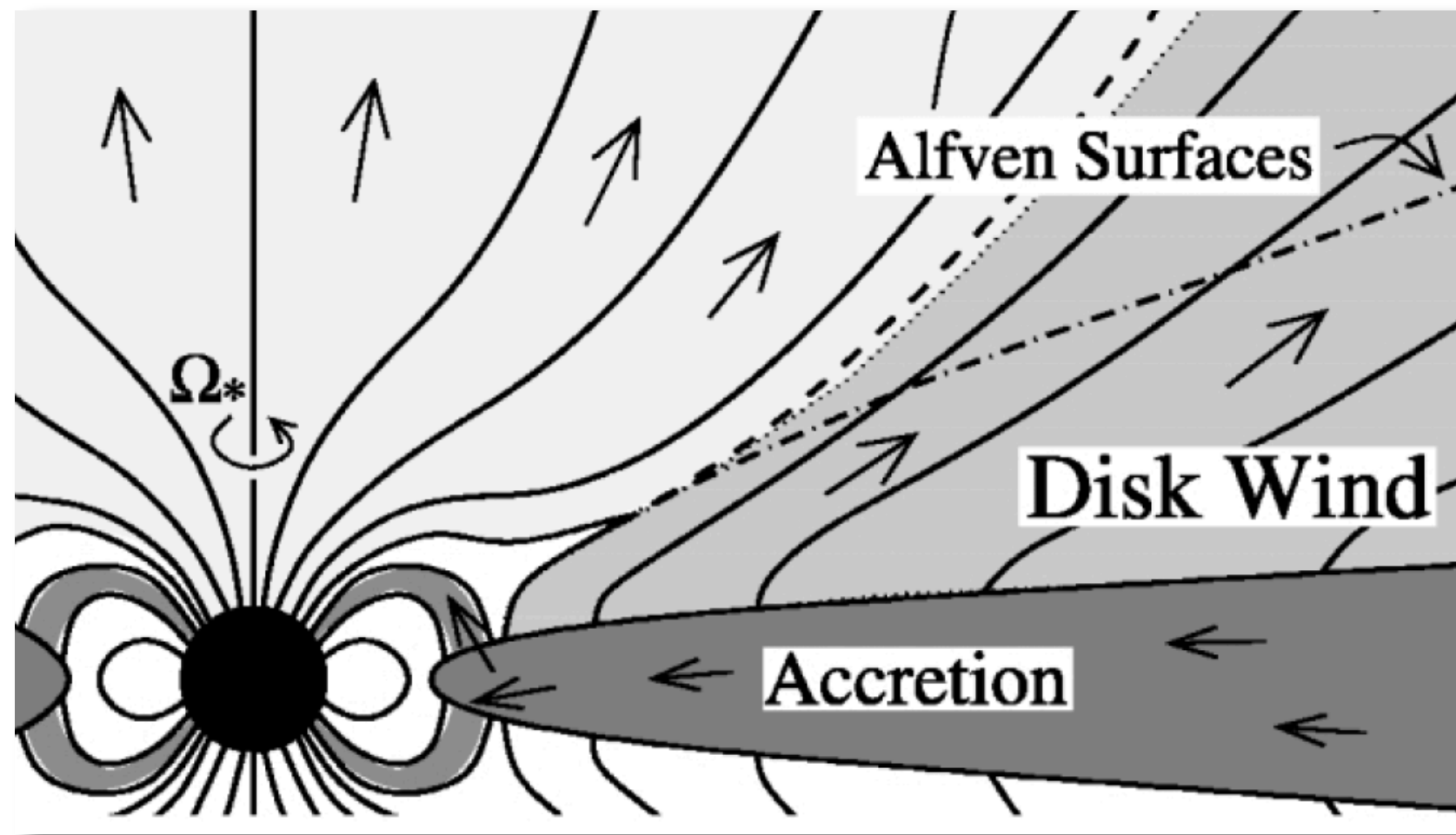
See a review by e.g. Romanova & Owocki 2015

Classical T Tauri stars are typical examples.

Today's topic: Importance of 3D effects

Previous 2D axisymmetric models

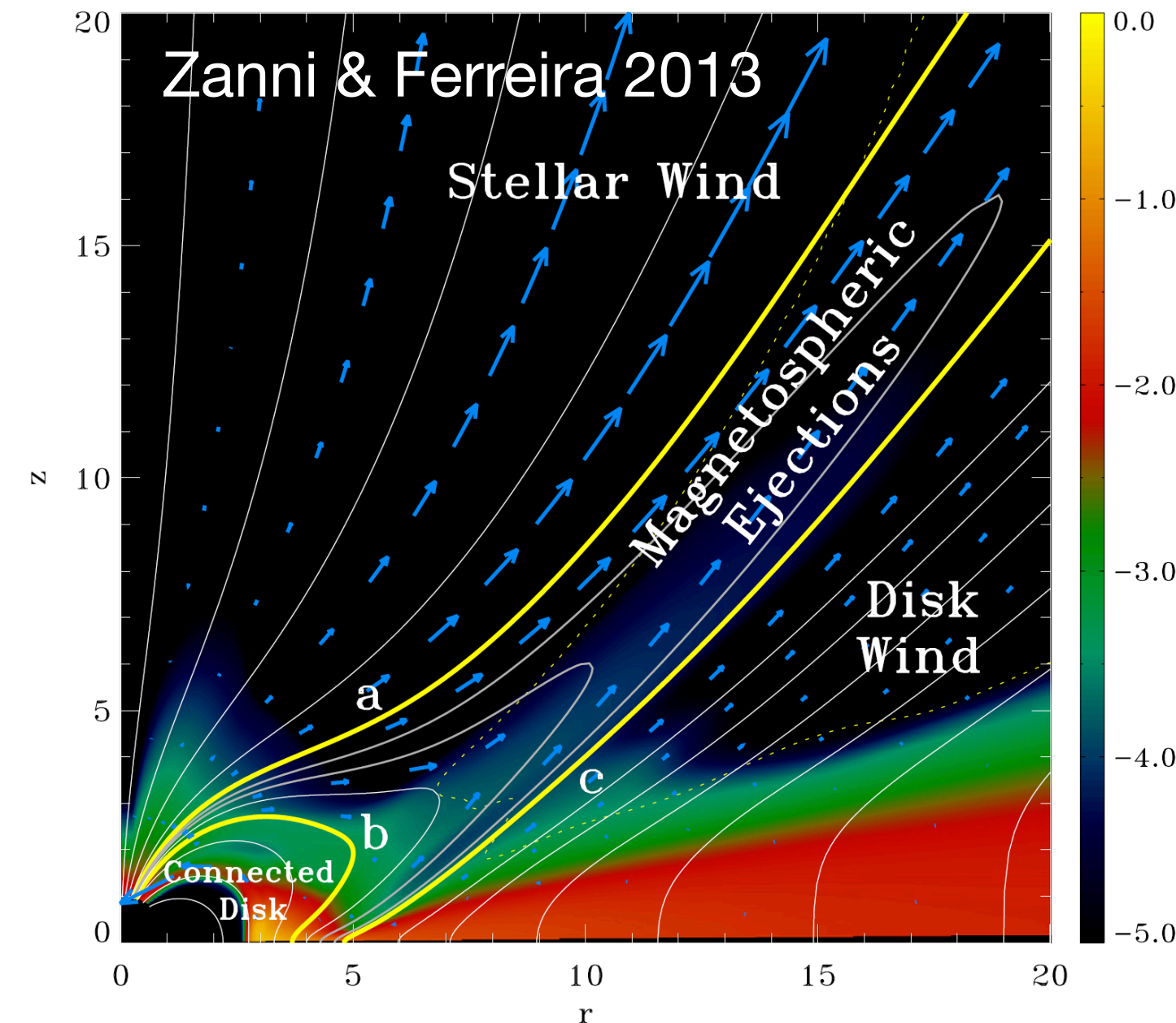
General accretion and outflow structures



Matt & Pudritz 2005

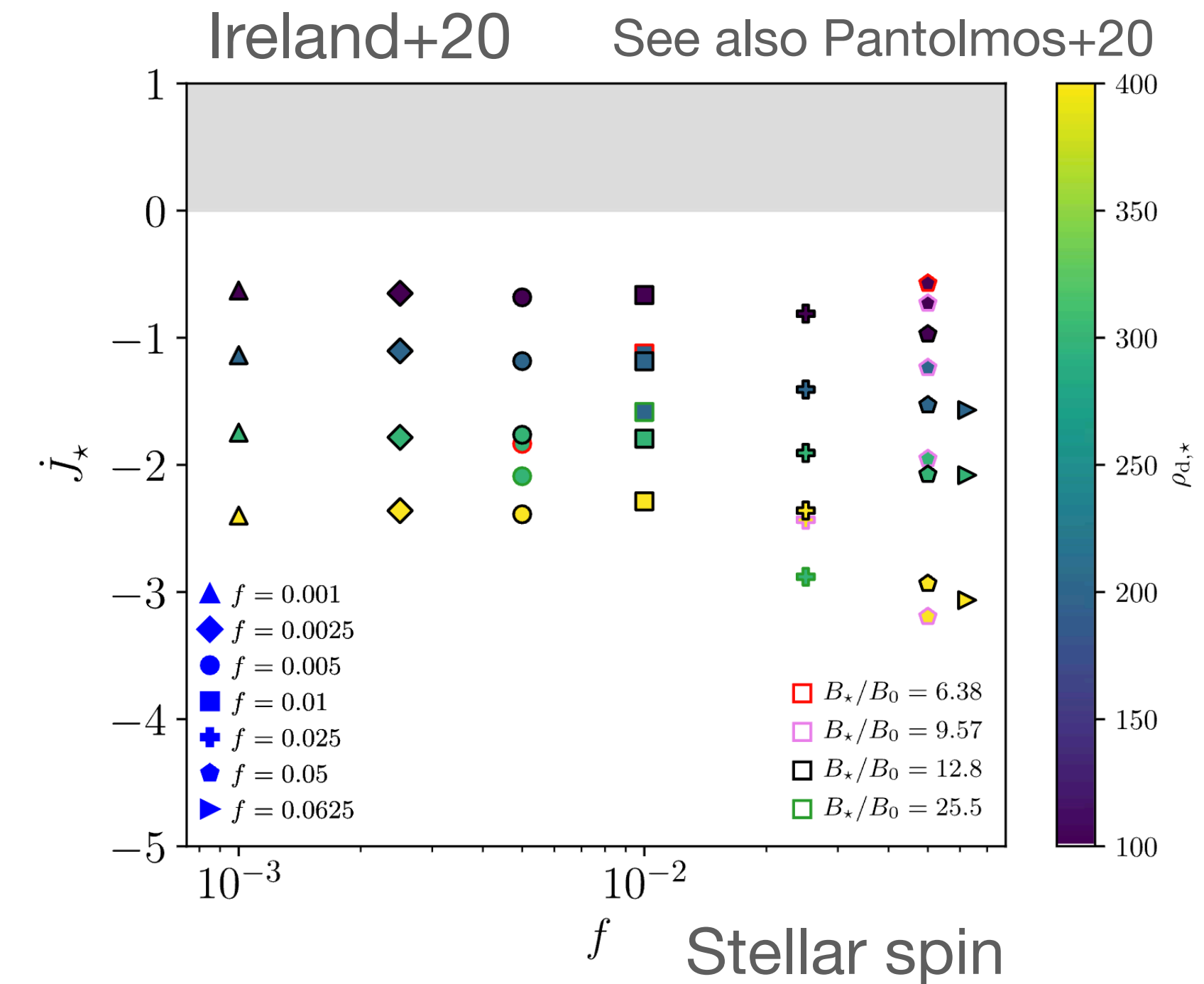
See also Ghosh & Lamb 79, Fendt 09

coronal mass ejections/flares



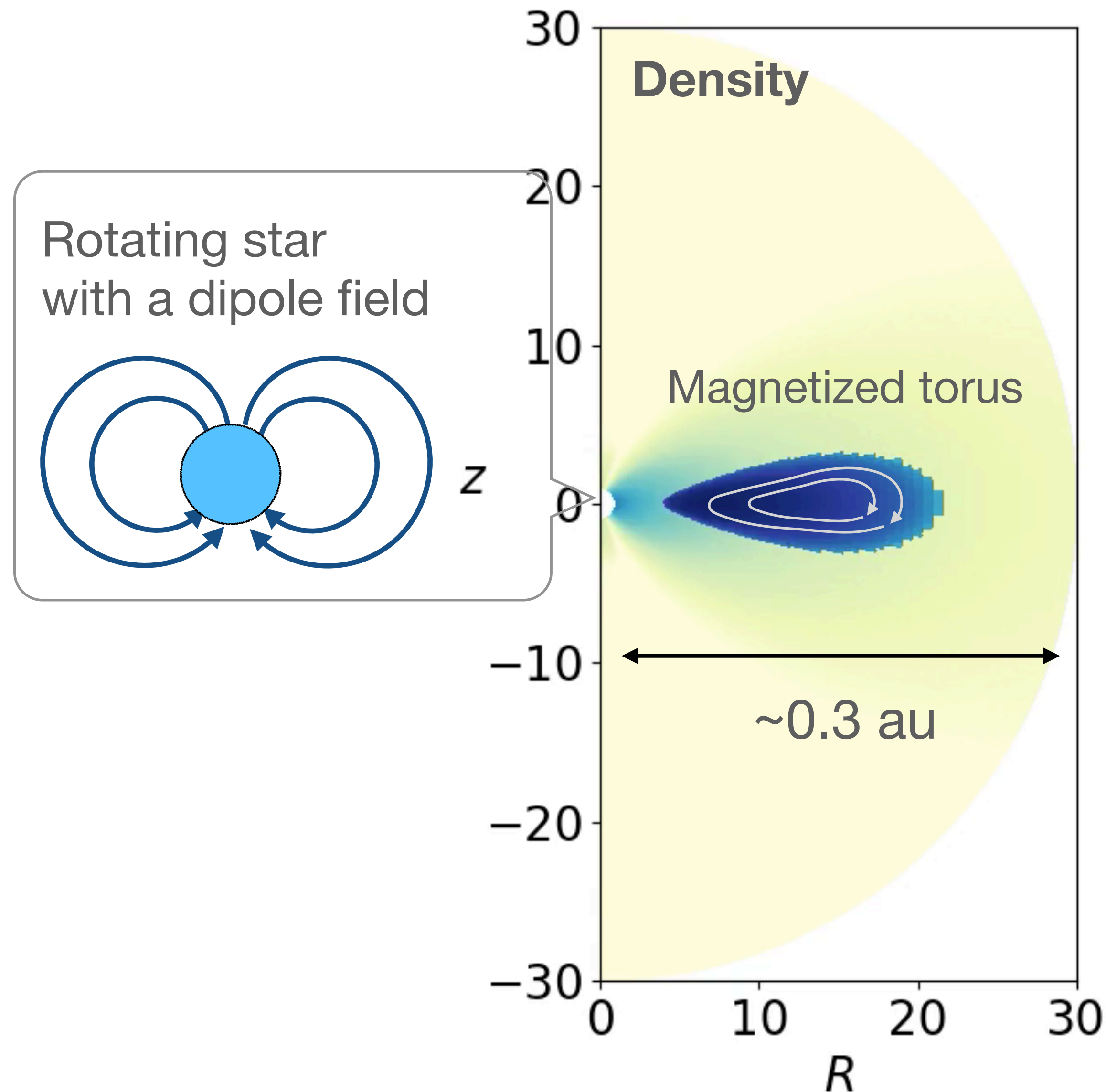
See also Shu+94, Hayashi+ 96, Ireland+12

spin-up/down torques



2D models have established a “standard picture” and enabled a wide range of parameter investigations.

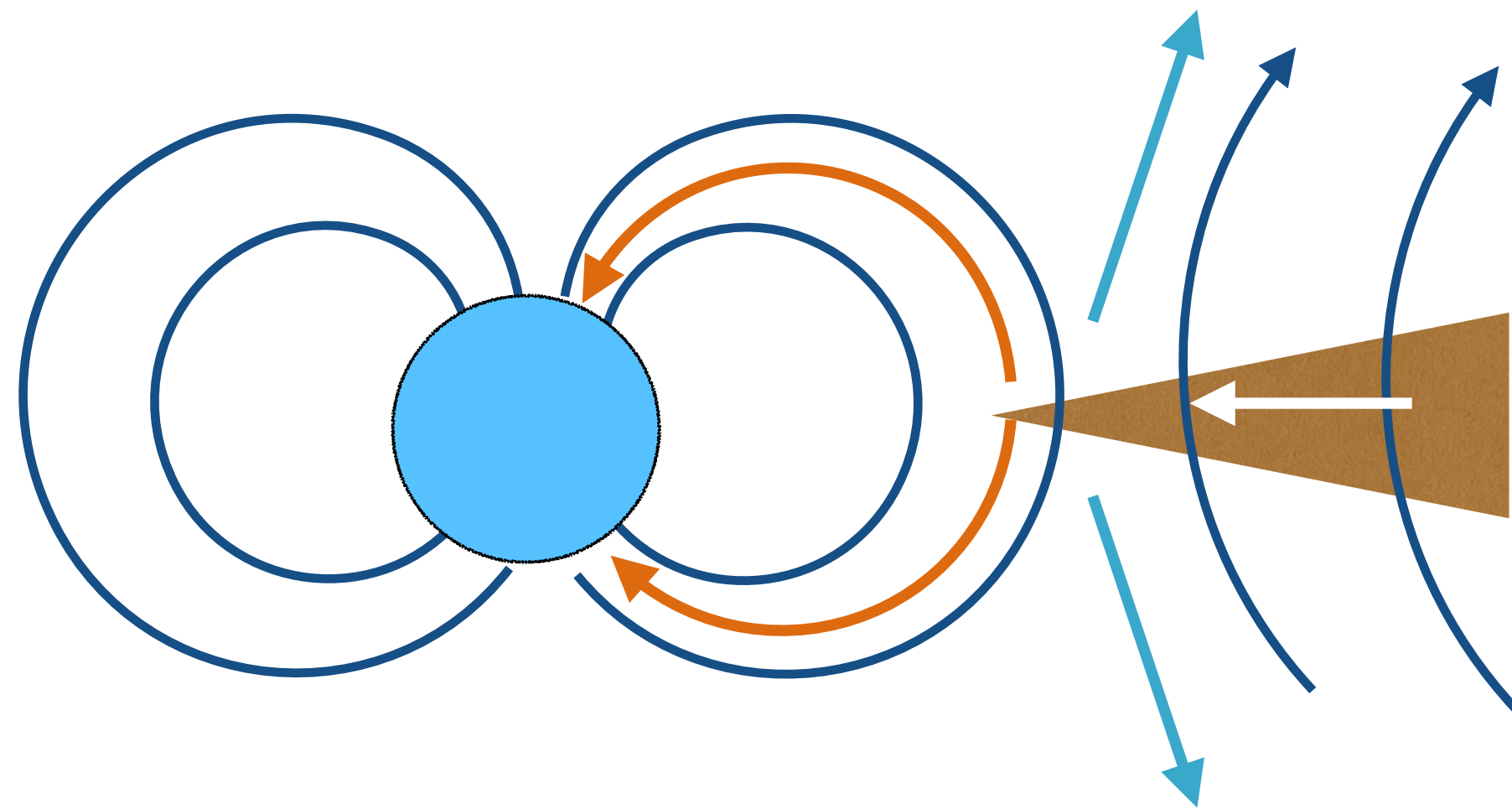
Model setup of our 3D models



- Spherical coordinates
- Resistive MHD simulations
- Radiation transfer is not solved. Locally isothermal in the disk.
- Stellar wind included.

2D vs 3D

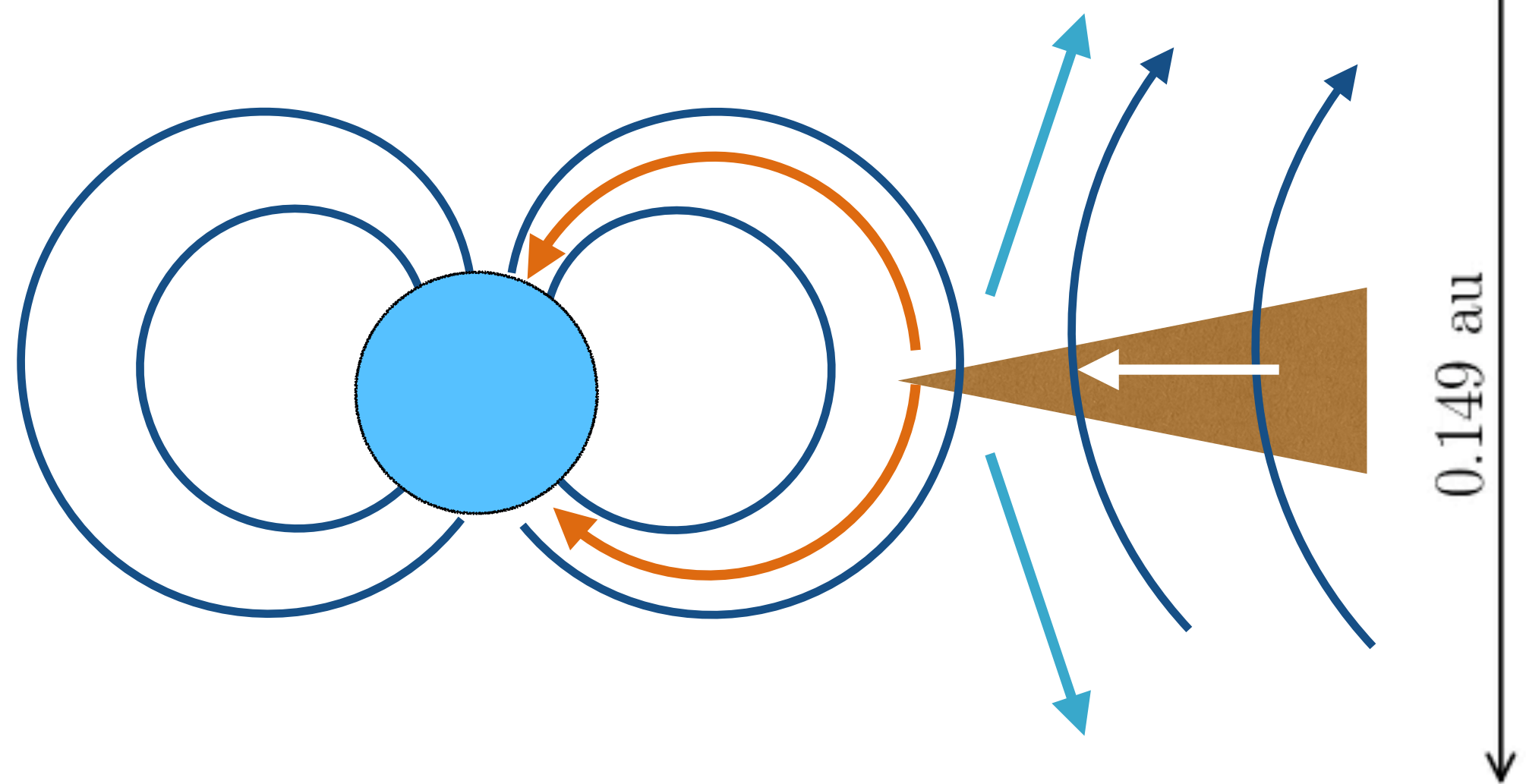
2D models



- Laminar flow structure
- Transition from midplane accretion to polar accretion
- Magnetosphere-disk interaction occurs via some effective resistivity.

2D vs 3D

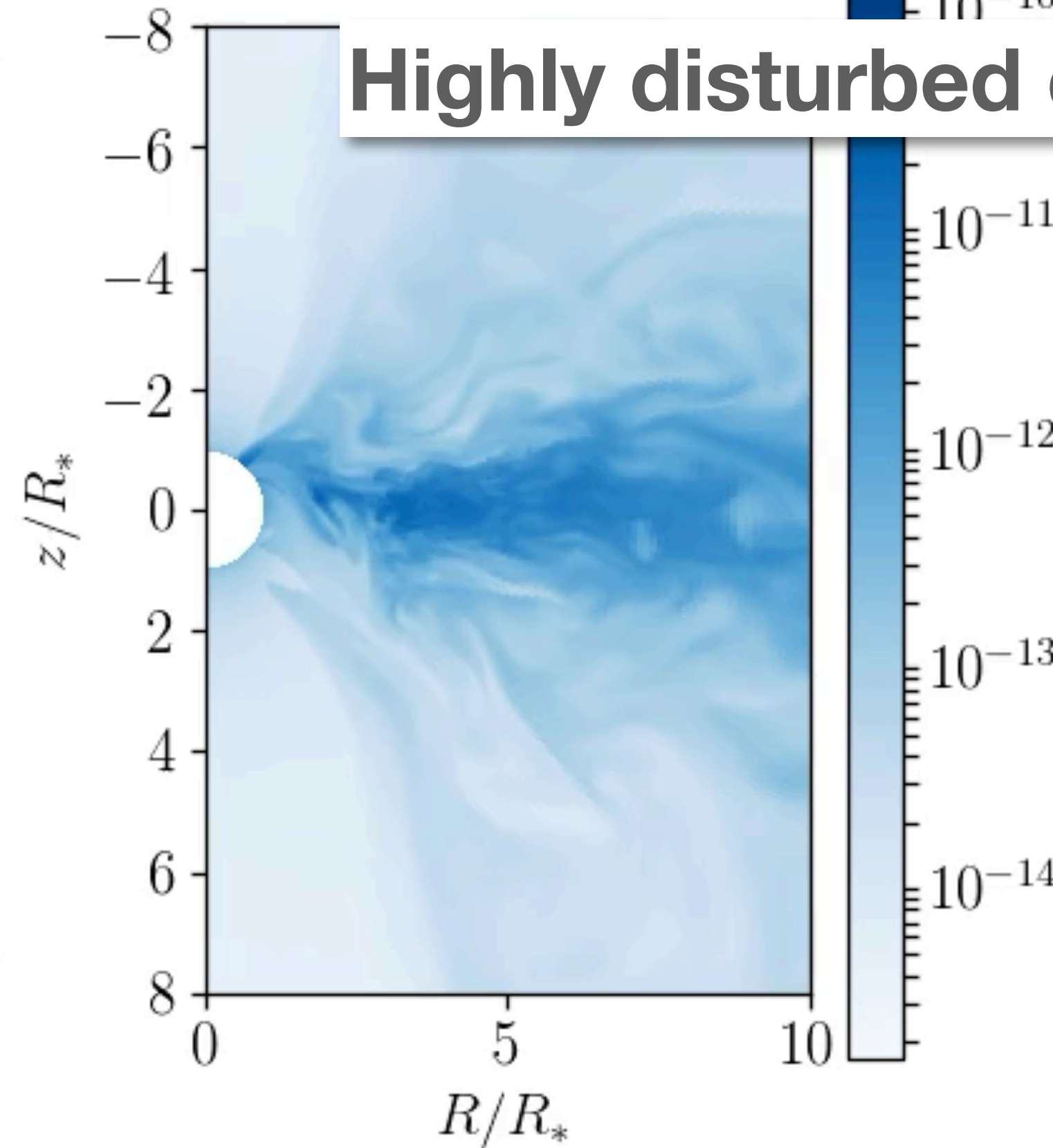
2D models



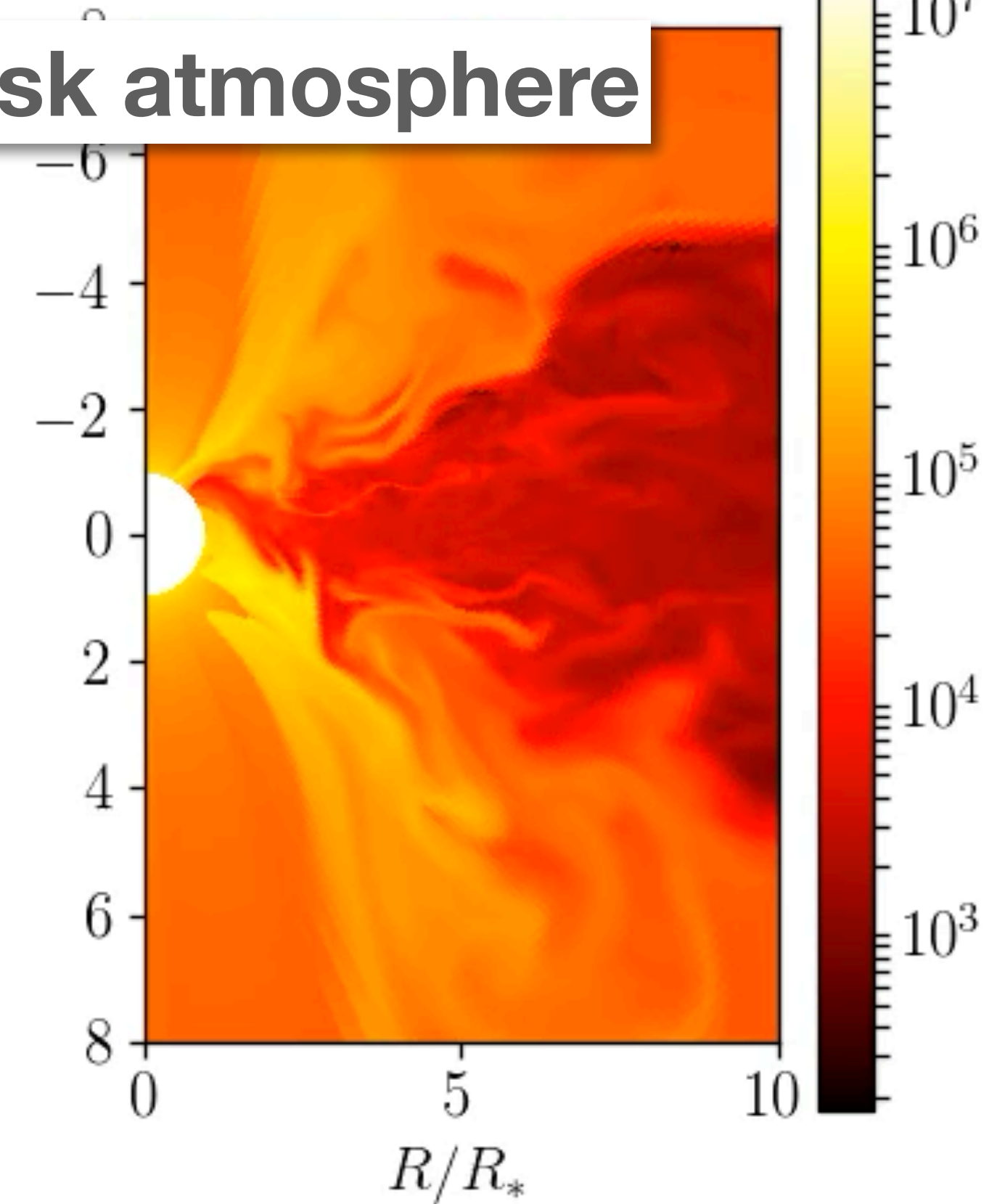
- Laminar flow structure
- Transition from midplane accretion to polar accretion
- Magnetosphere-disk interaction occurs via some effective resistivity.

3D model (ST+22)

Density



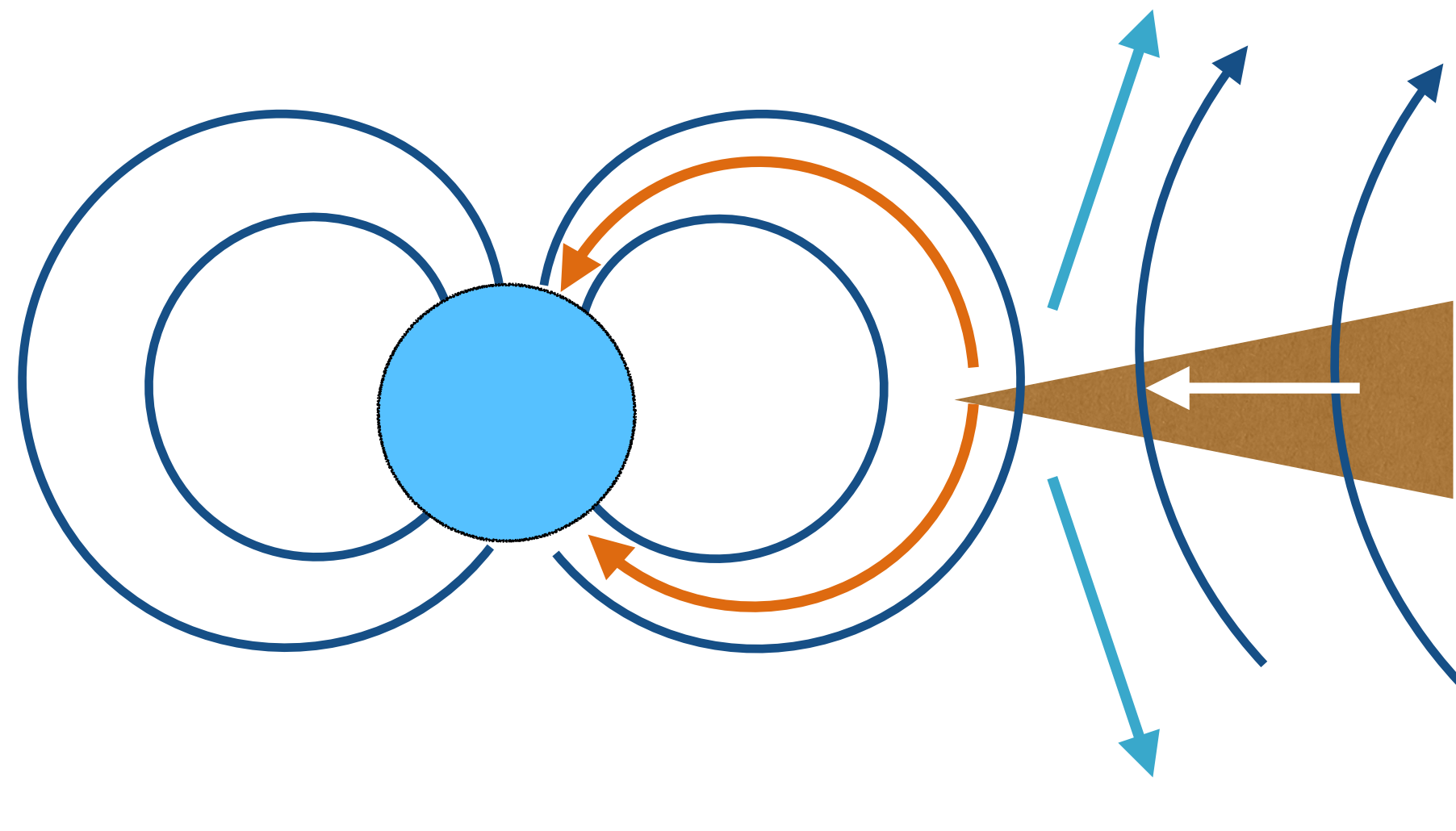
Temperature



Highly disturbed disk atmosphere

2D vs 3D

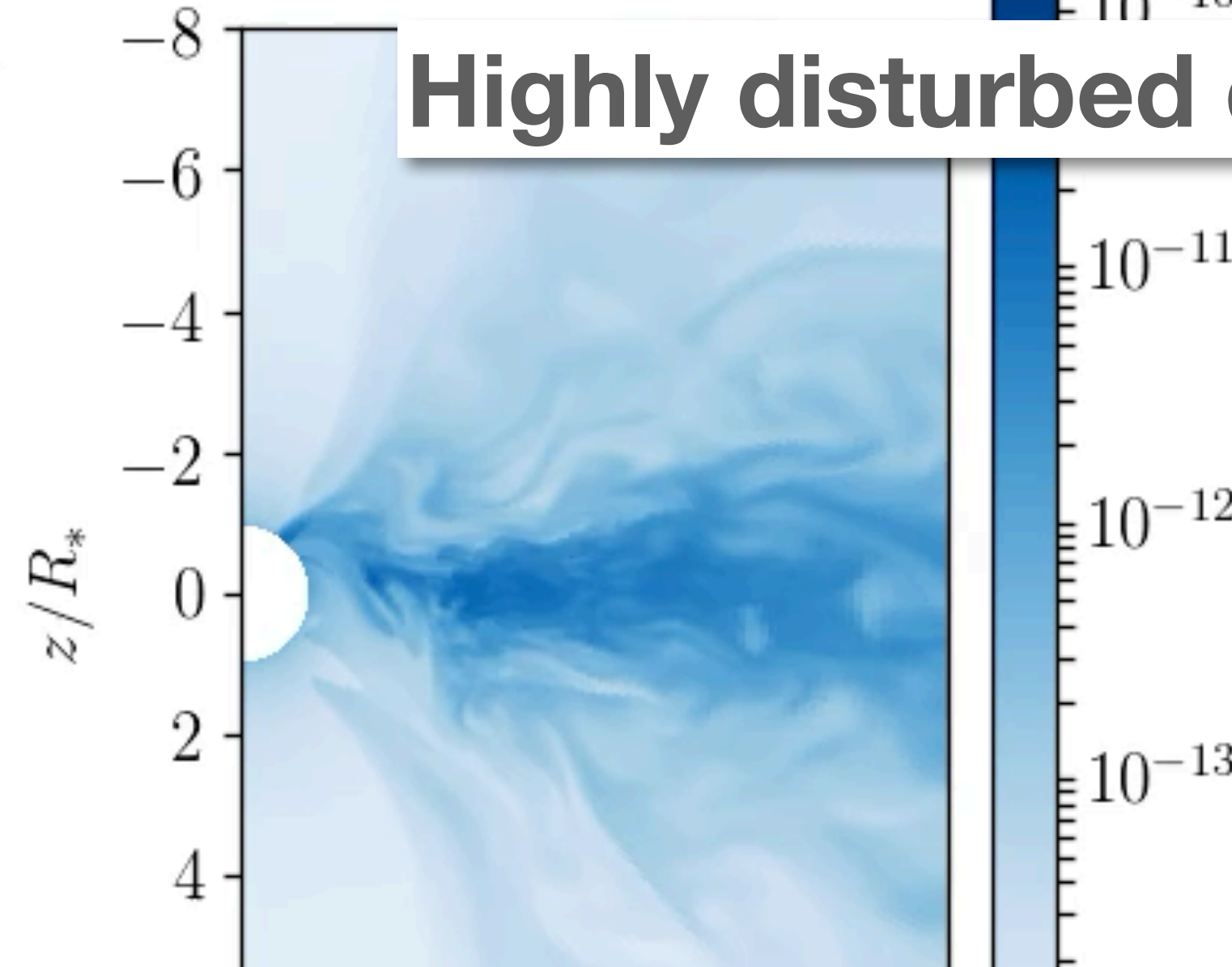
2D models



- Laminar flow structure
- Transition from midplane accretion to polar accretion
- Magnetosphere-disk interaction occurs via some effective resistivity.

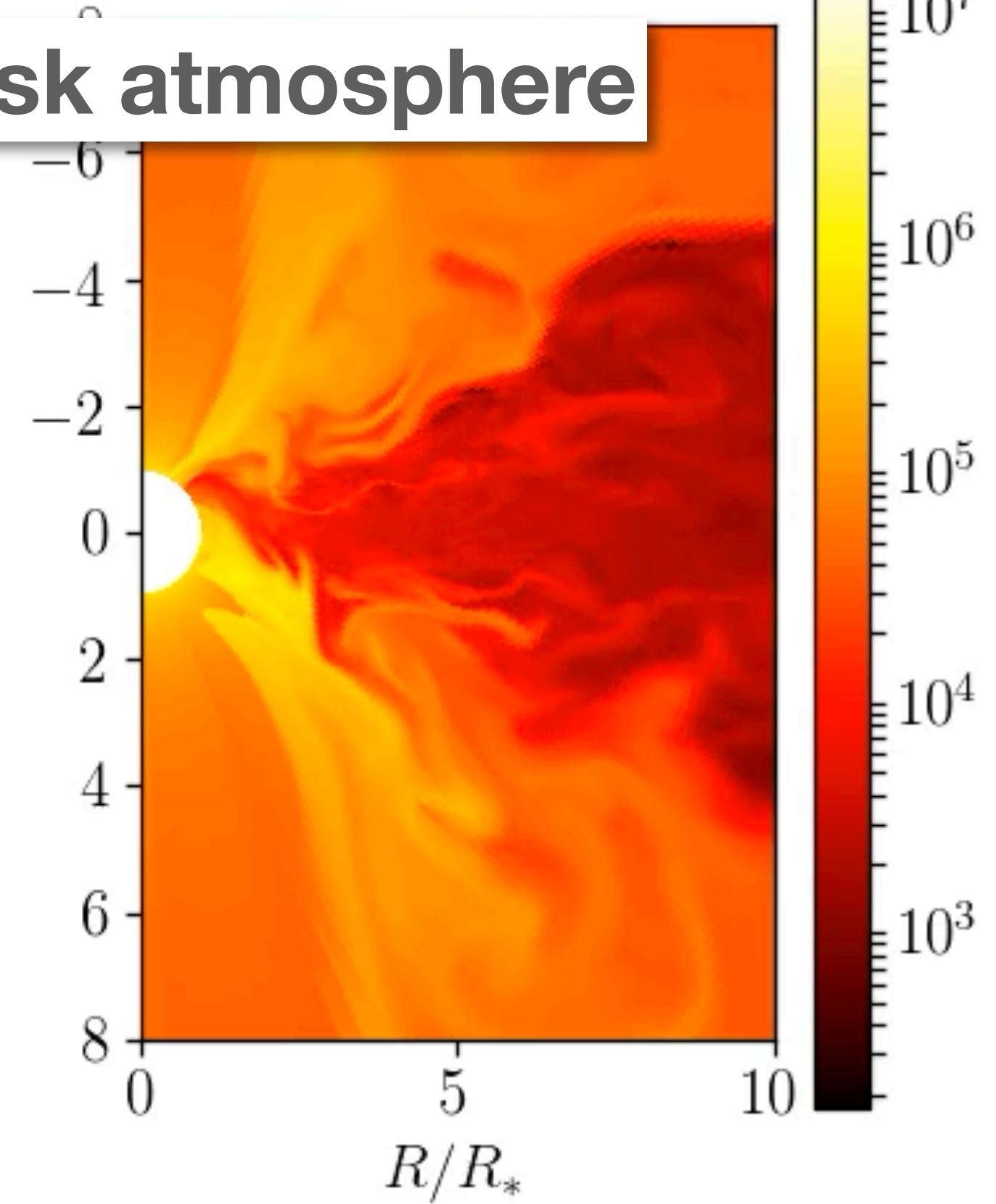
3D model (ST+22)

Density

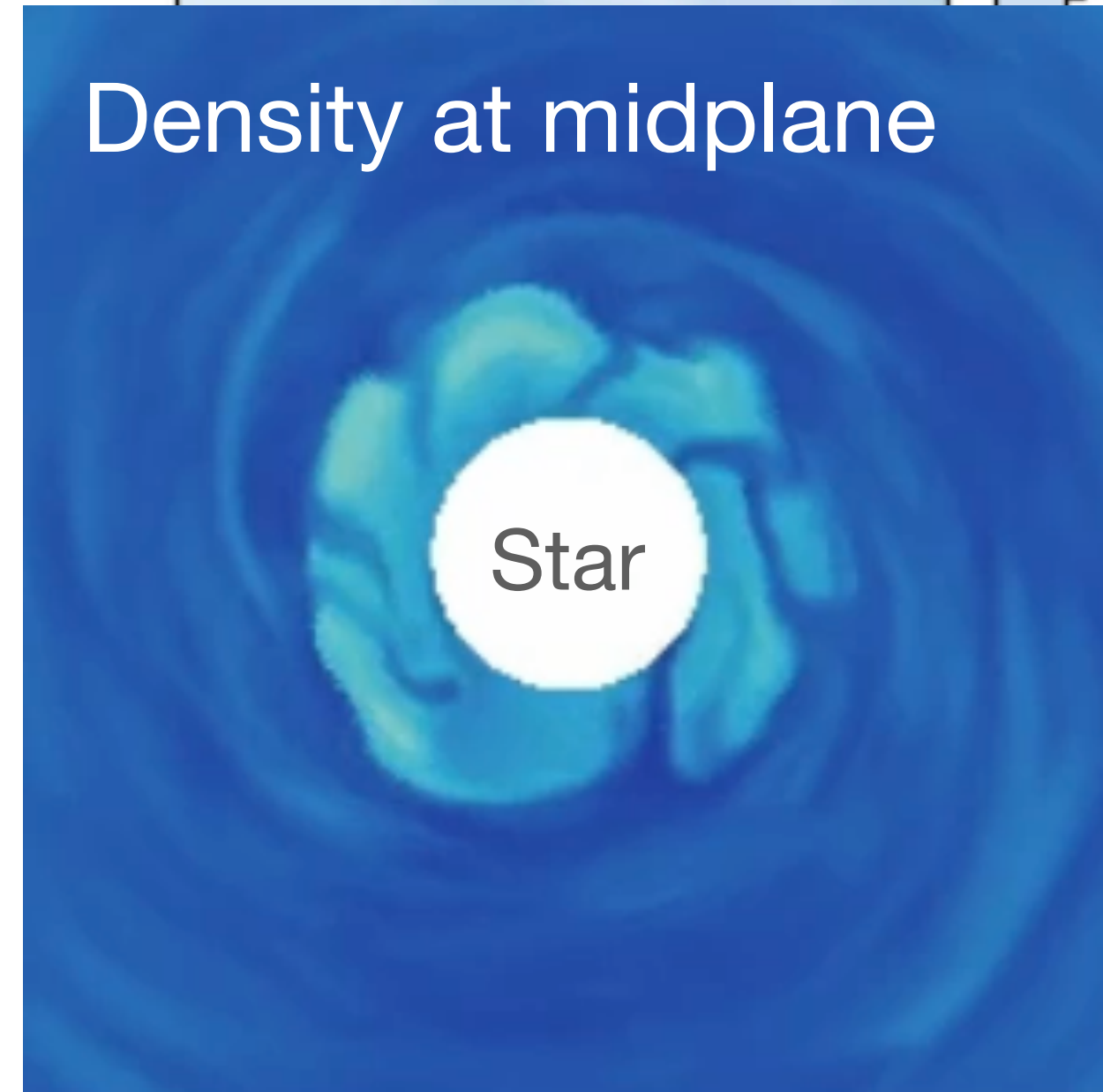


Highly disturbed disk atmosphere

Temperature



Density at midplane



Penetrating flows in the magnetosphere

Stehle & Spruit 01, Blinova+16

3D model (ST+22)

Density

Temperature

Highly disturbed disk atmosphere

Importance
of these 3D structures?

0.149 au

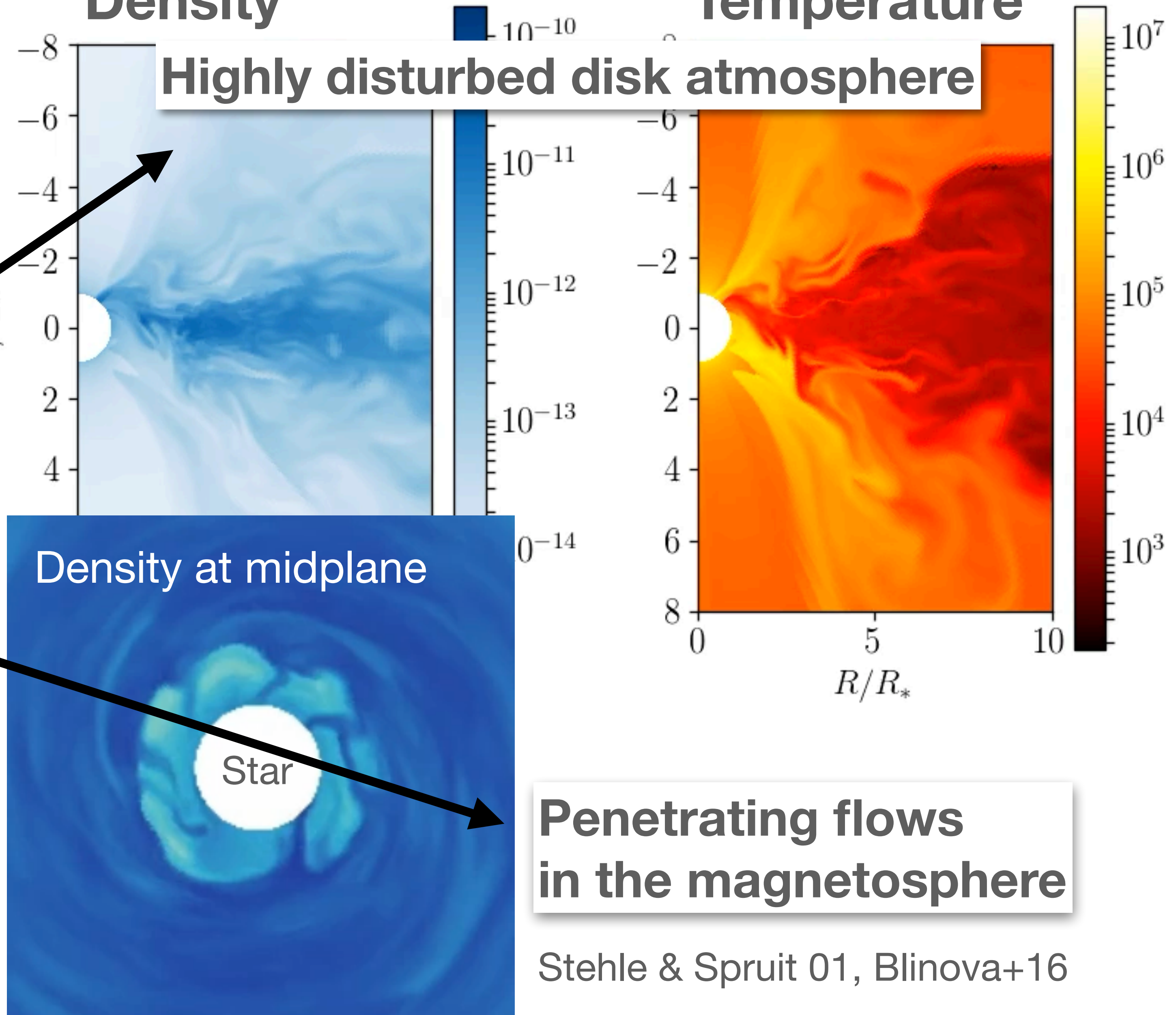
z/R_*

Density at midplane

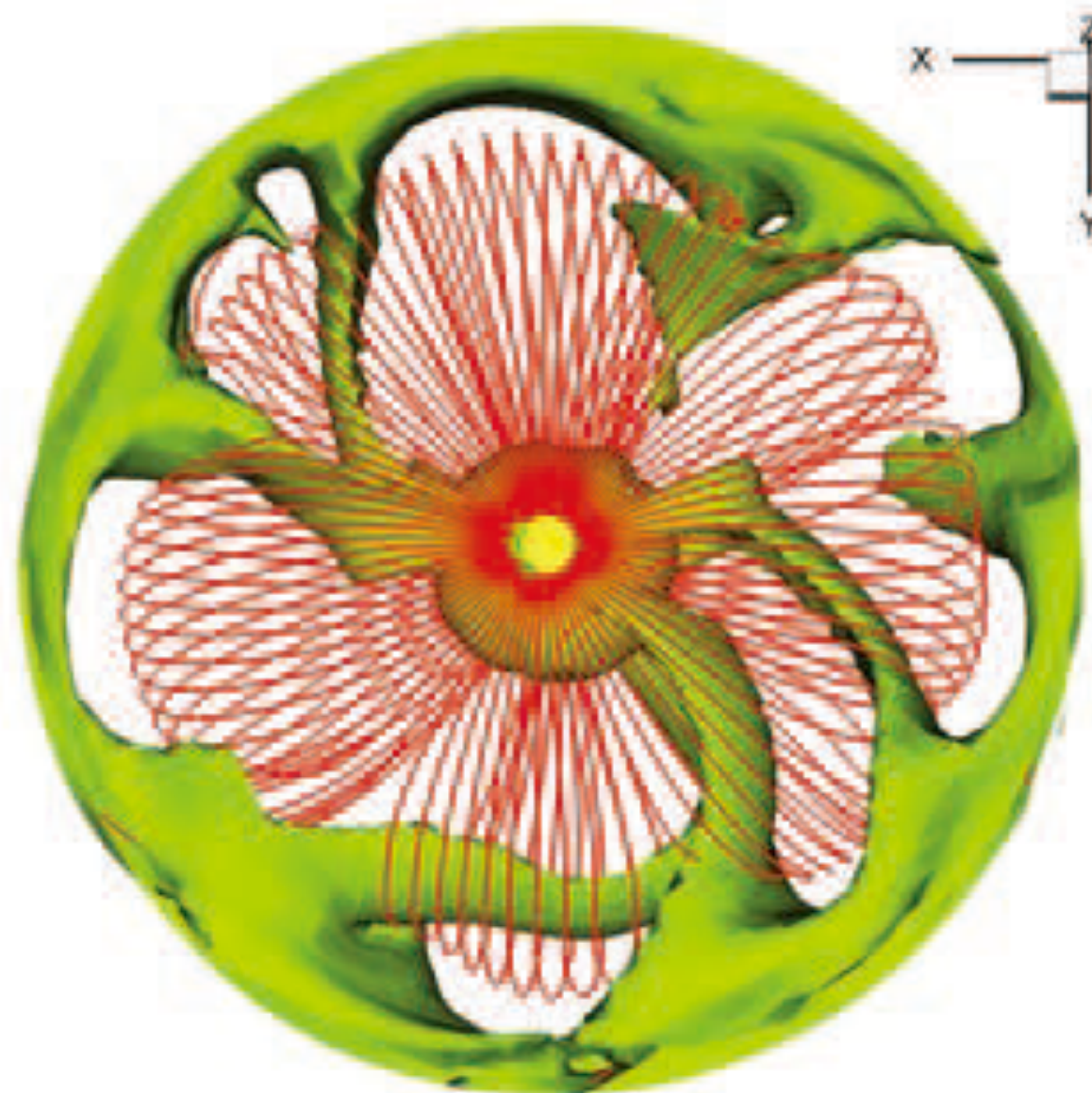
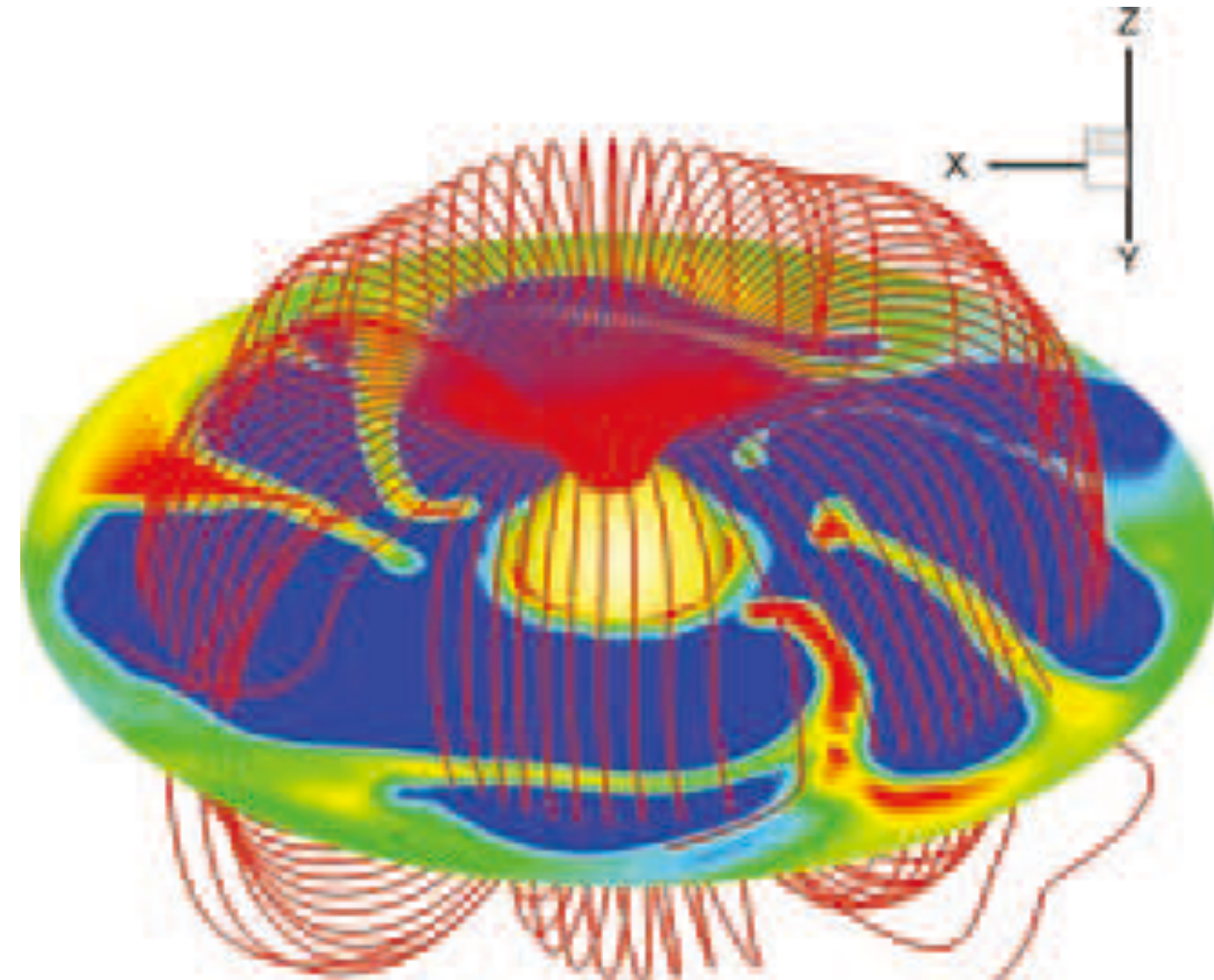
Star

Penetrating flows
in the magnetosphere

Stehle & Spruit 01, Blinova+16



Magnetic Rayleigh-Taylor instability



Criterion for the development of the instability
(Spruit et al. 95)

$$\underbrace{\gamma_{B\Sigma}^2 \equiv -g_{\text{eff}} \frac{d}{dr} \ln \frac{\Sigma}{B_z}}_{\text{Destabilizing by gravity \& magnetic field}} > \underbrace{2 \left(r \frac{d\Omega}{dr} \right)^2}_{\text{Stabilizing by the velocity shear}} \equiv \gamma_{\Omega}^2,$$

Destabilizing
by gravity & magnetic field

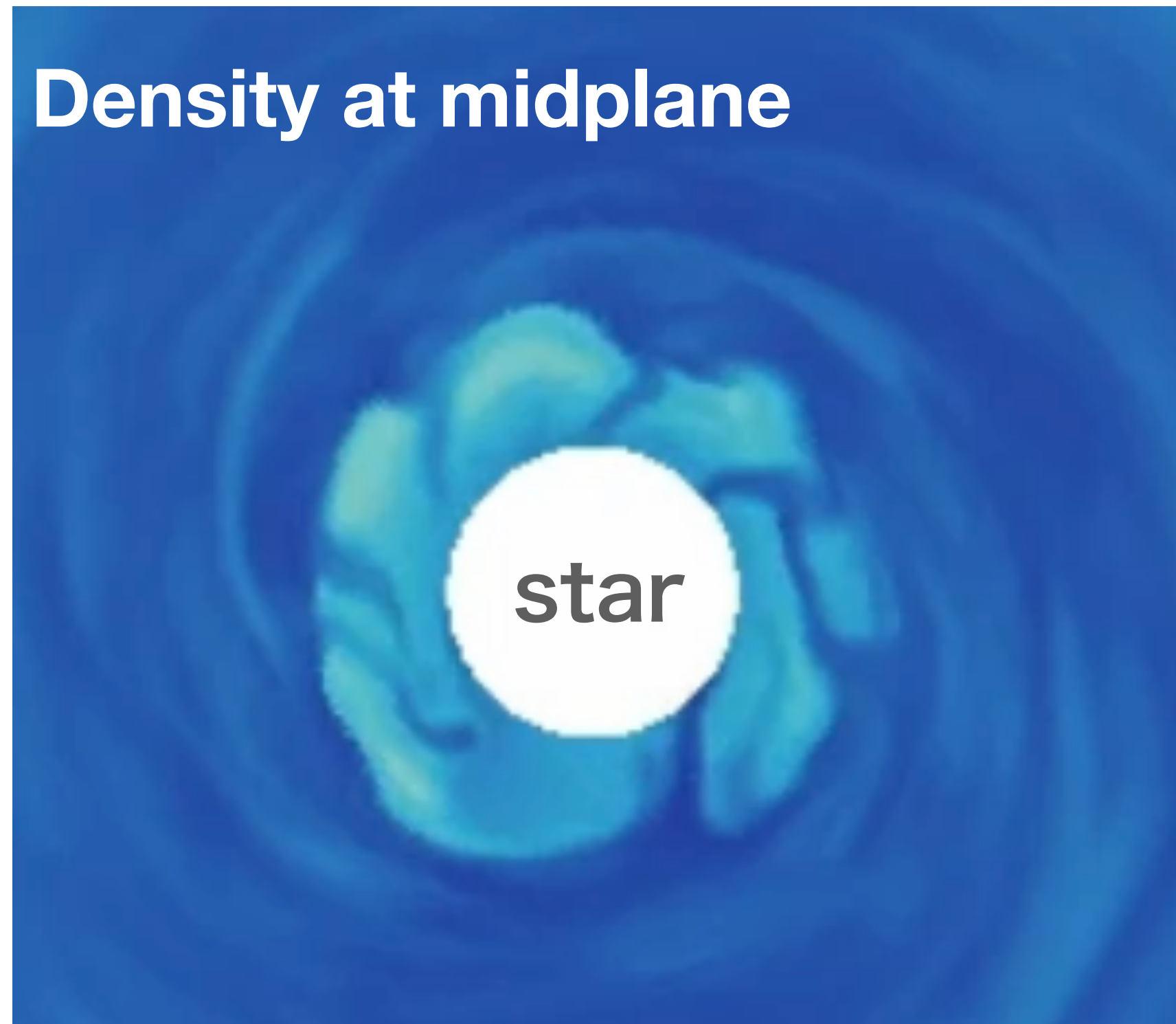
Stabilizing
by the velocity shear

$$g_{\text{eff}} \equiv - \left[\Omega_K(r)^2 - \langle \Omega(r) \rangle^2 \right] r$$

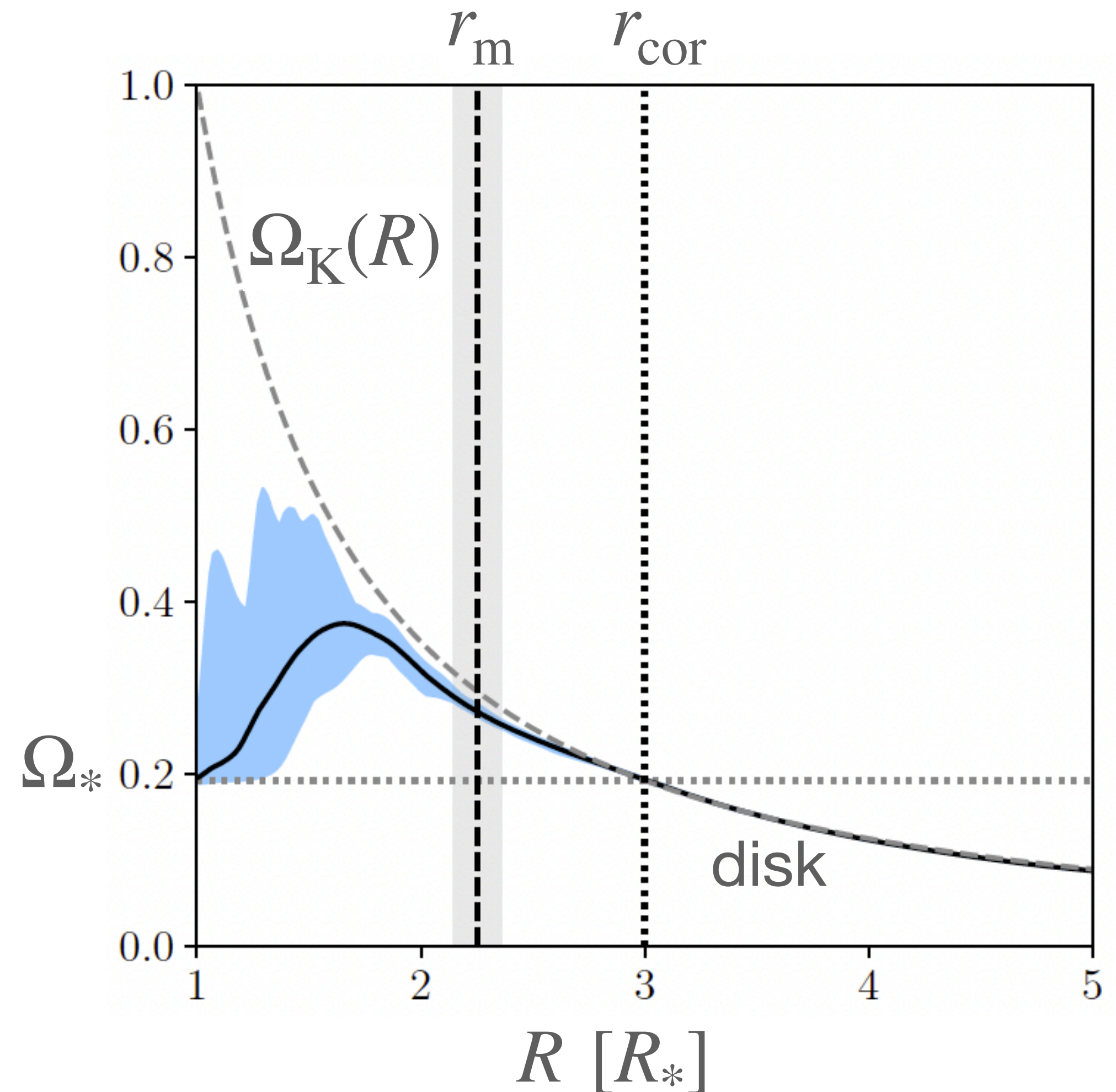
Effective gravitational acceleration

The finger structures are more prominent
in more slowly rotating stars.

Penetrating flows and rotation profile



Penetrating flows continue to rotate at \sim Keplerian speed until they lose angular momenta
—> **They force to rotate the surrounding magnetic field together.**

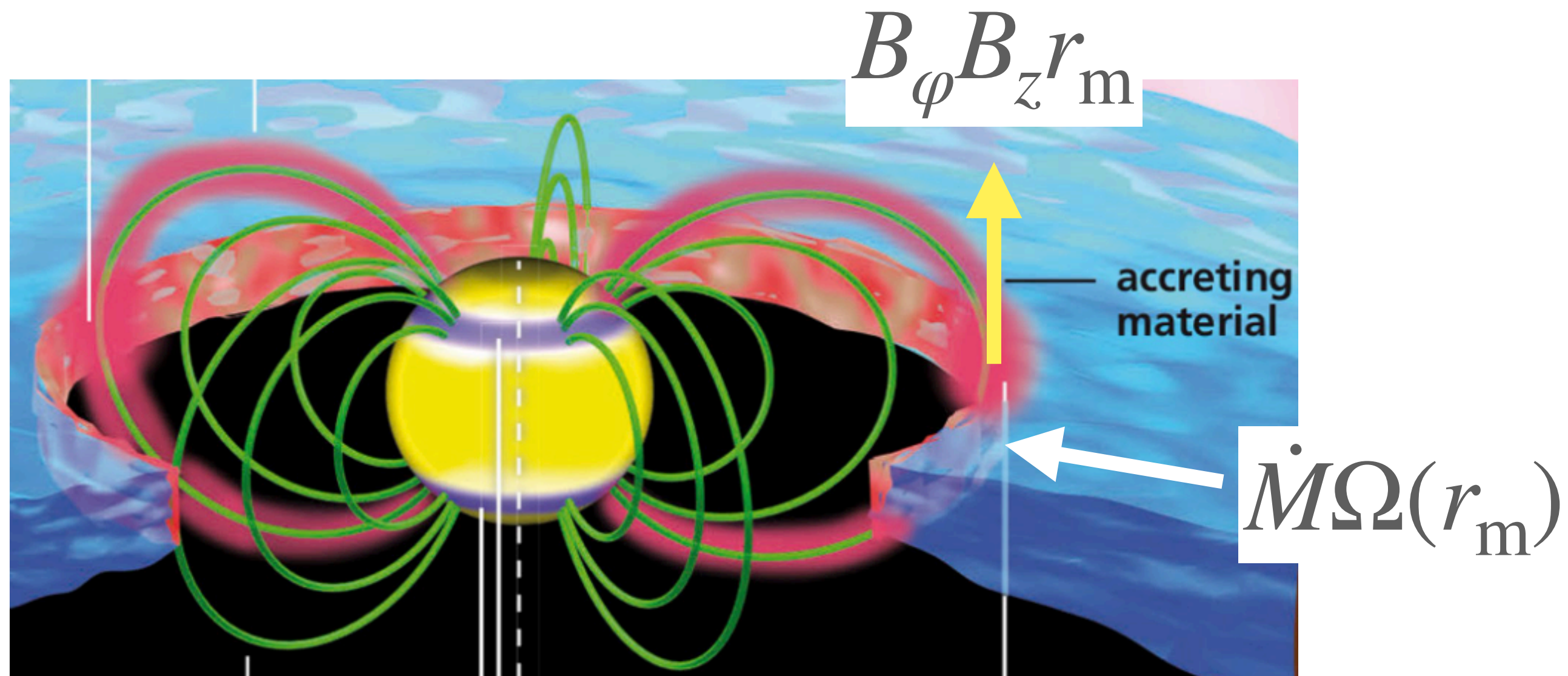


See also Kluzniak & Rappaport 2007

Magnetospheric radius

The steady angular momentum transfer eq:

$$\dot{M}\Omega(r_m) \approx B_\phi B_z r_m$$



3D sim: $\Omega(r_m) = \Omega_K(r_m)$ (Kepler rot.)

↓

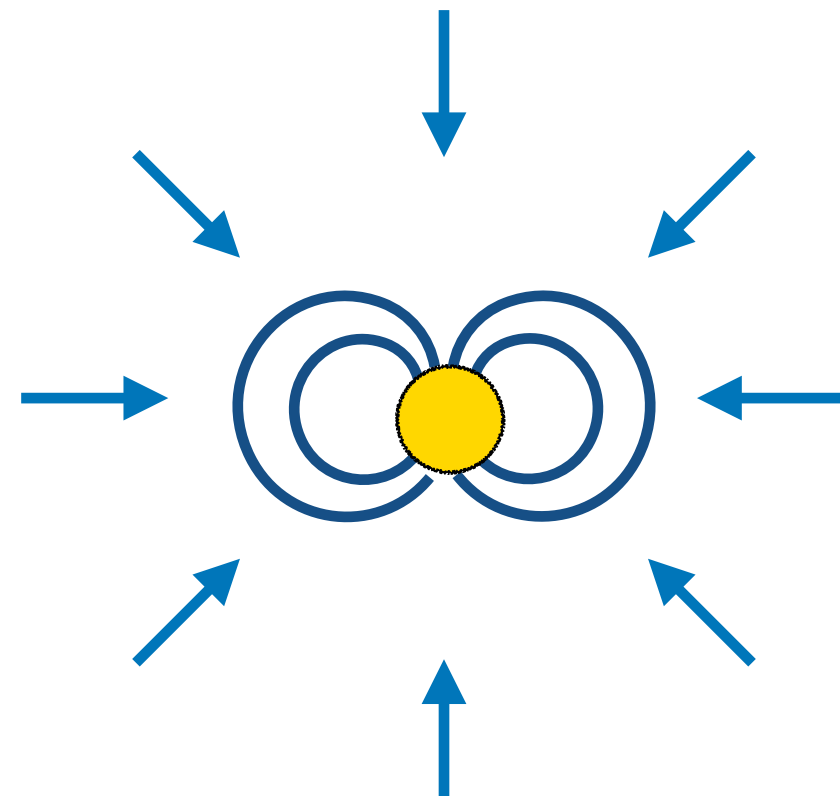
$$r_m \approx \eta'^{2/7} \left(\frac{\mu_*^4}{GM_* \dot{M}^2} \right)^{1/7}$$
$$\mu_* \equiv B_* R_*^3, \quad \eta' = |B_\phi / B_z|$$

For other formulae based on 2D models,
see e.g. Bessolaz+08, D'Angelo & Spruit 10

Magnetospheric radius

Commonly used formula

Ghosh & Lamb 1978, 1979, Königl 1991



The diagram shows a central yellow circle representing a star, surrounded by two concentric blue circles representing the magnetosphere. Eight blue arrows point radially inward from all directions toward the central star, representing the inflow of material in spherical accretion.


$$\rho v_r^2 \approx \frac{B^2}{8\pi}$$

in the spherical accretion flows

$$r_{\text{m,GL}} \approx \left(\frac{\mu_*^4}{2GM_*\dot{M}^2} \right)^{1/7}$$

Observations suggest that this relation works well even for disk accretion (e.g. Gravity collab. 20).
Why?

3D sim: $\Omega(r_{\text{m}}) = \Omega_{\text{K}}(r_{\text{m}})$ (Kepler rot.)



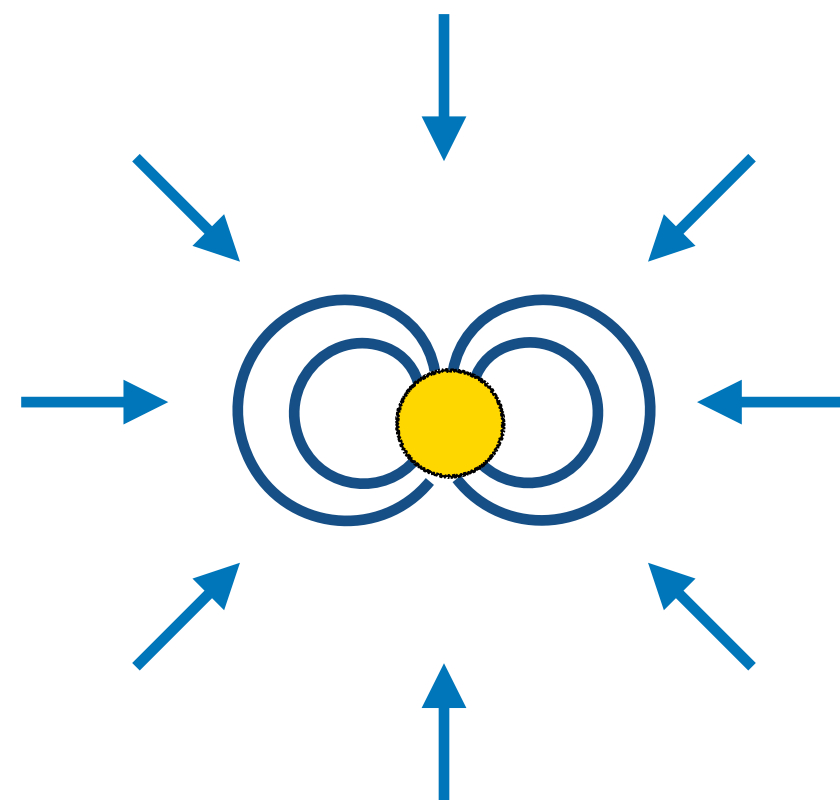
A large grey arrow pointing downwards, indicating a logical consequence or derivation.

$$r_{\text{m}} \approx \eta'^{2/7} \left(\frac{\mu_*^4}{GM_*\dot{M}^2} \right)^{1/7}$$
$$\mu_* \equiv B_* R_*^3, \quad \eta' = |B_\phi / B_z|$$

Magnetospheric radius

Commonly used formula

Ghosh & Lamb 1978, 1979, Königl 1991



The diagram shows a central yellow circle representing a star, surrounded by two concentric blue circles representing the magnetosphere. Eight blue arrows point radially inward from all directions toward the star, representing spherical accretion flows.


$$\rho v_r^2 \approx \frac{B^2}{8\pi}$$

in the spherical accretion flows

$$r_{\text{m,GL}} \approx \left(\frac{\mu_*^4}{2GM_*\dot{M}^2} \right)^{1/7}$$

Observations suggest that this relation works well even for disk accretion (e.g. Gravity collab. 20).
Why?

3D sim: $\Omega(r_{\text{m}}) = \Omega_{\text{K}}(r_{\text{m}})$ (Kepler rot.)



A large grey arrow pointing downwards, indicating a derivation or consequence of the 3D simulation result.

$$r_{\text{m}} \approx \eta'^{2/7} \left(\frac{\mu_*^4}{GM_*\dot{M}^2} \right)^{1/7} \approx r_{\text{m,GL}}$$
$$\mu_* \equiv B_* R_*^3, \quad \eta' = |B_\phi / B_z|$$

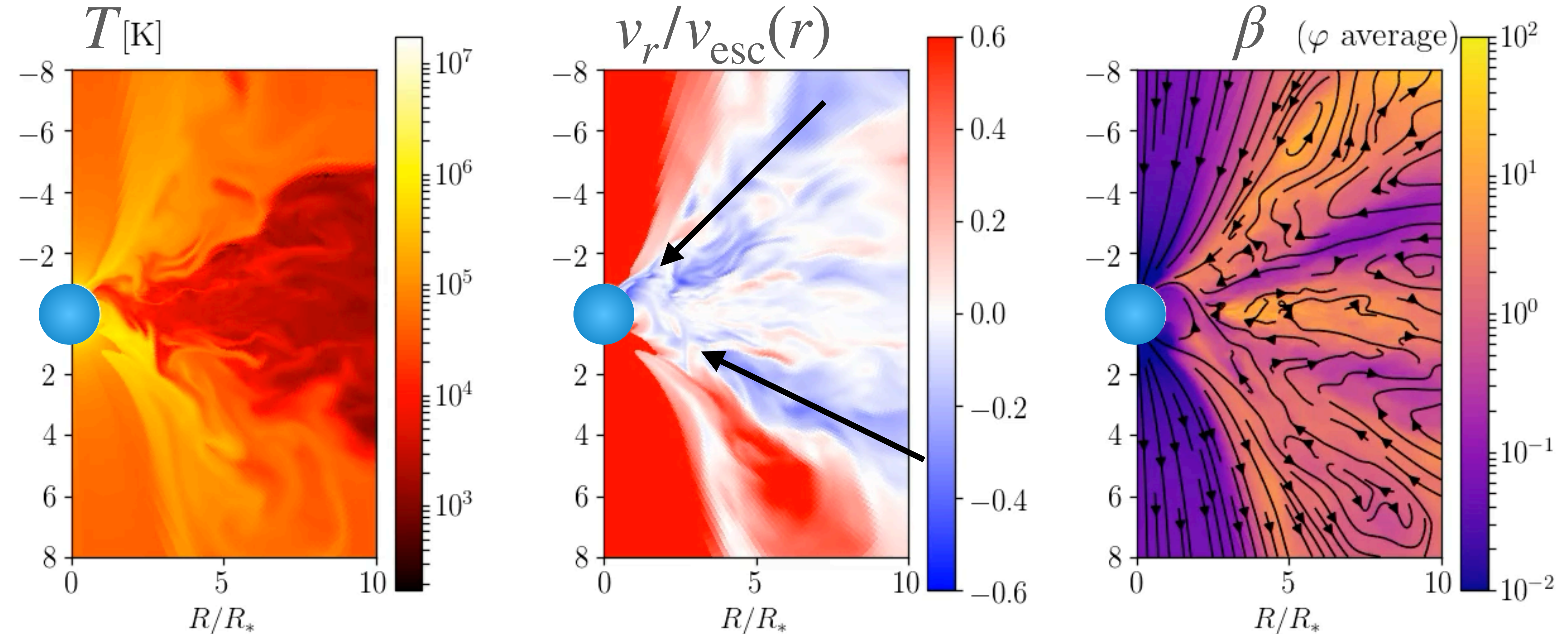
Ghosh-Lamb-like relation can be derived from the angular momentum transfer eq. for disk accretion (ST+22)

Penetrating flows are important for determining the magnetospheric radius.

Fluctuating atmosphere above MRI-turbulent disk

MRI-turbulent disks produce **failed disk wind (disk surface acc)**.

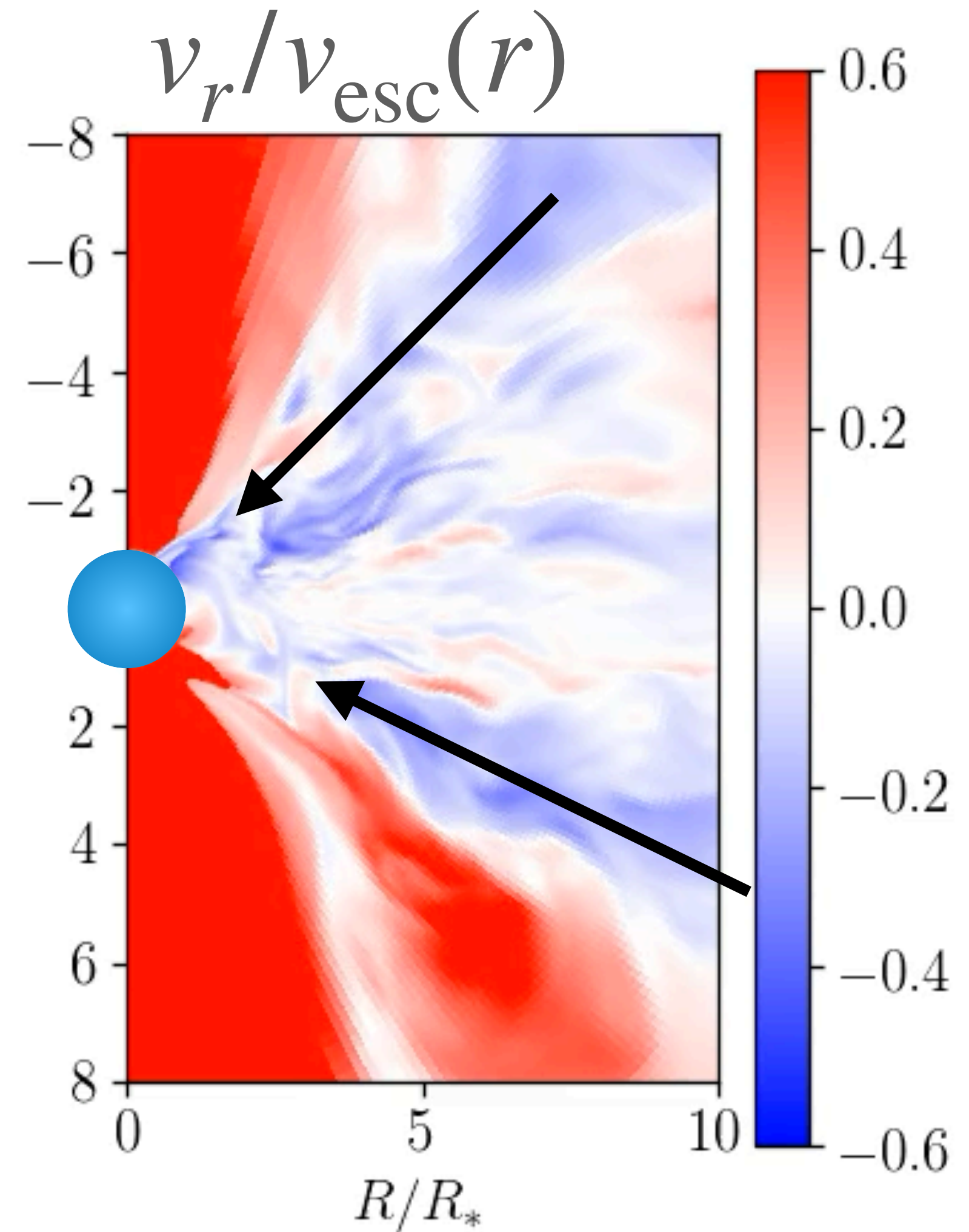
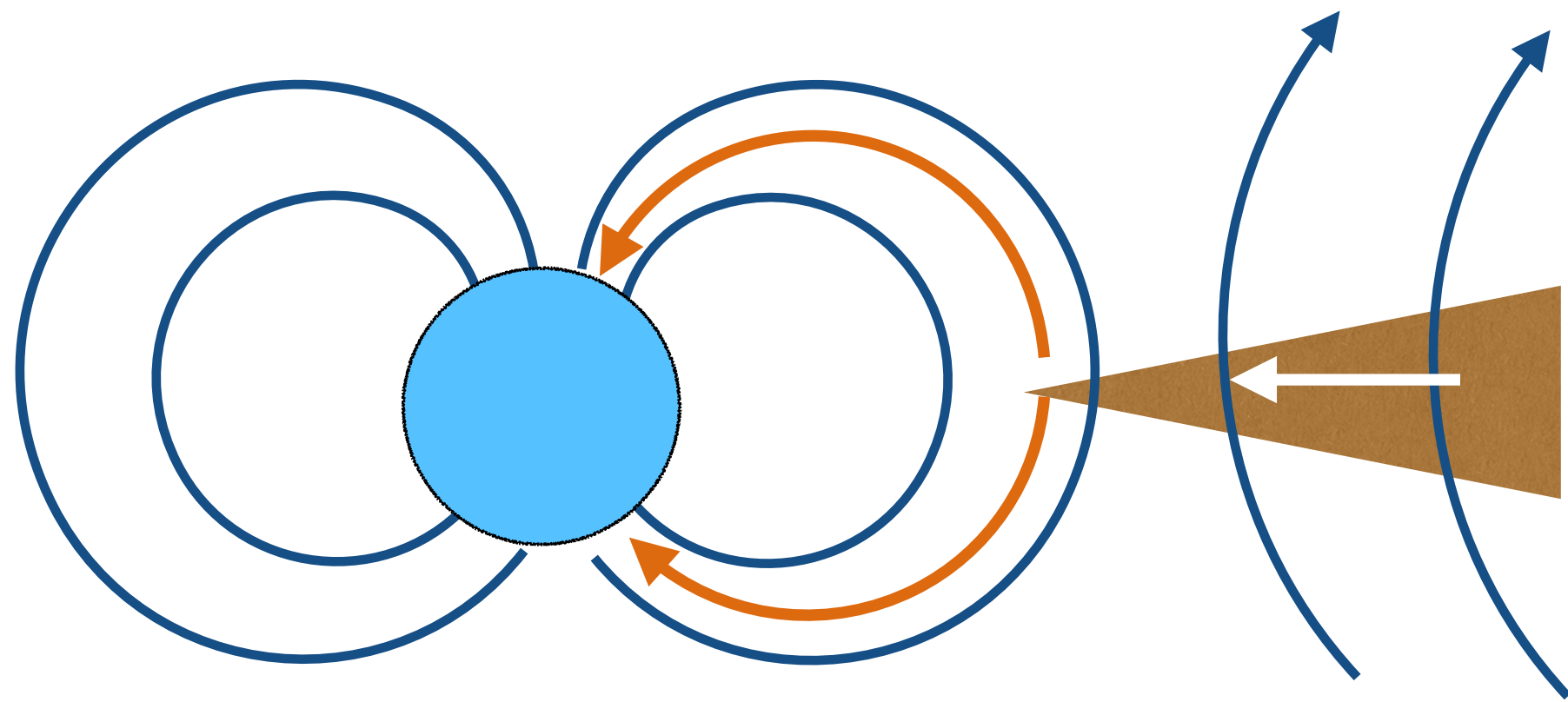
(e.g. ST+18, Zhu & Stone 18, Jacquemin-Ide+21)



Comparison: accretion flow structure

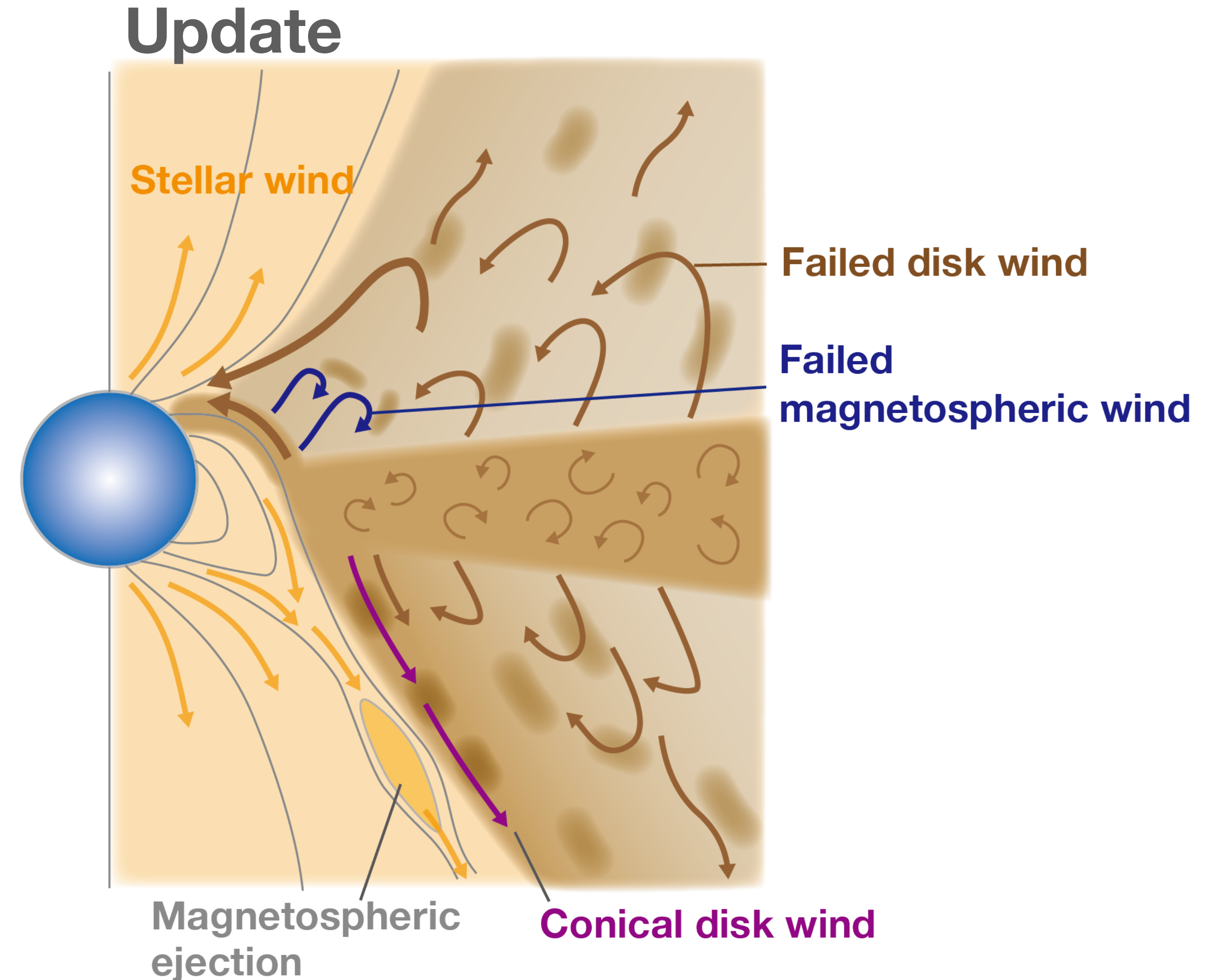
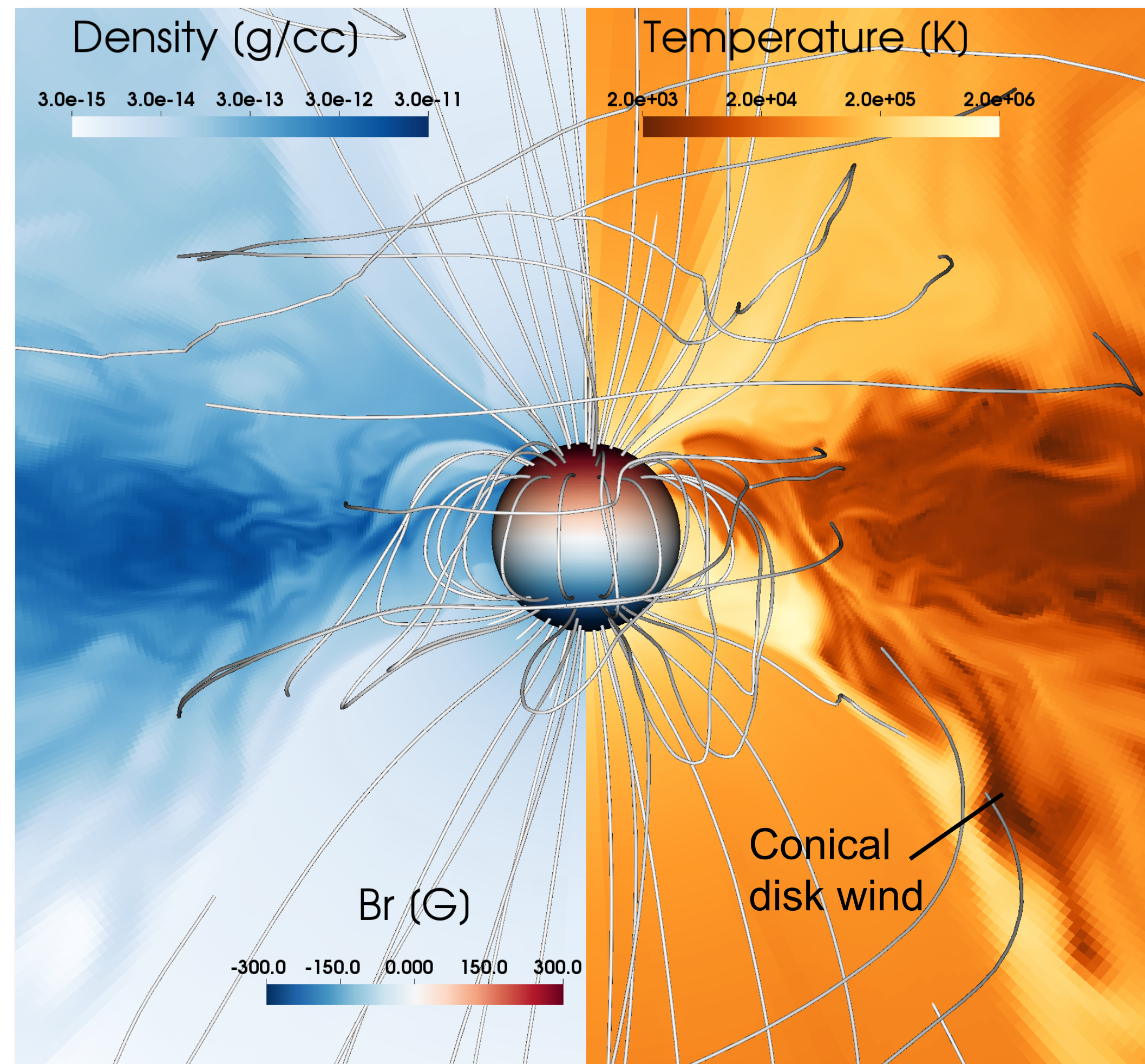
Polar accretion = classical magnetospheric acc. + **failed disk wind (disk surface acc)**

Classical magnetospheric accretion

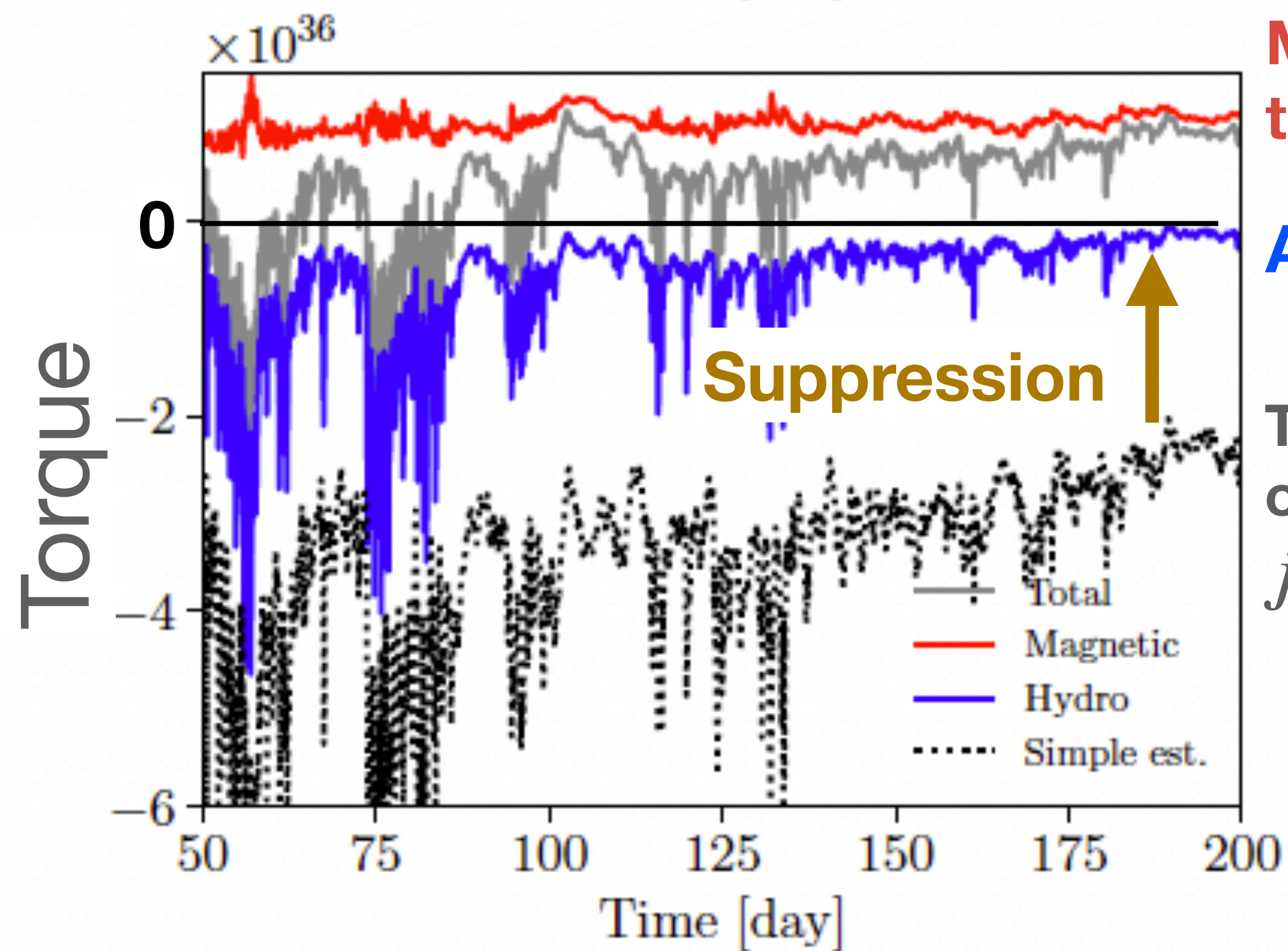


Comparison: accretion flow structure

Polar accretion = classical magnetospheric acc. + **failed disk wind (disk surface acc)**



Comments on accretion torque

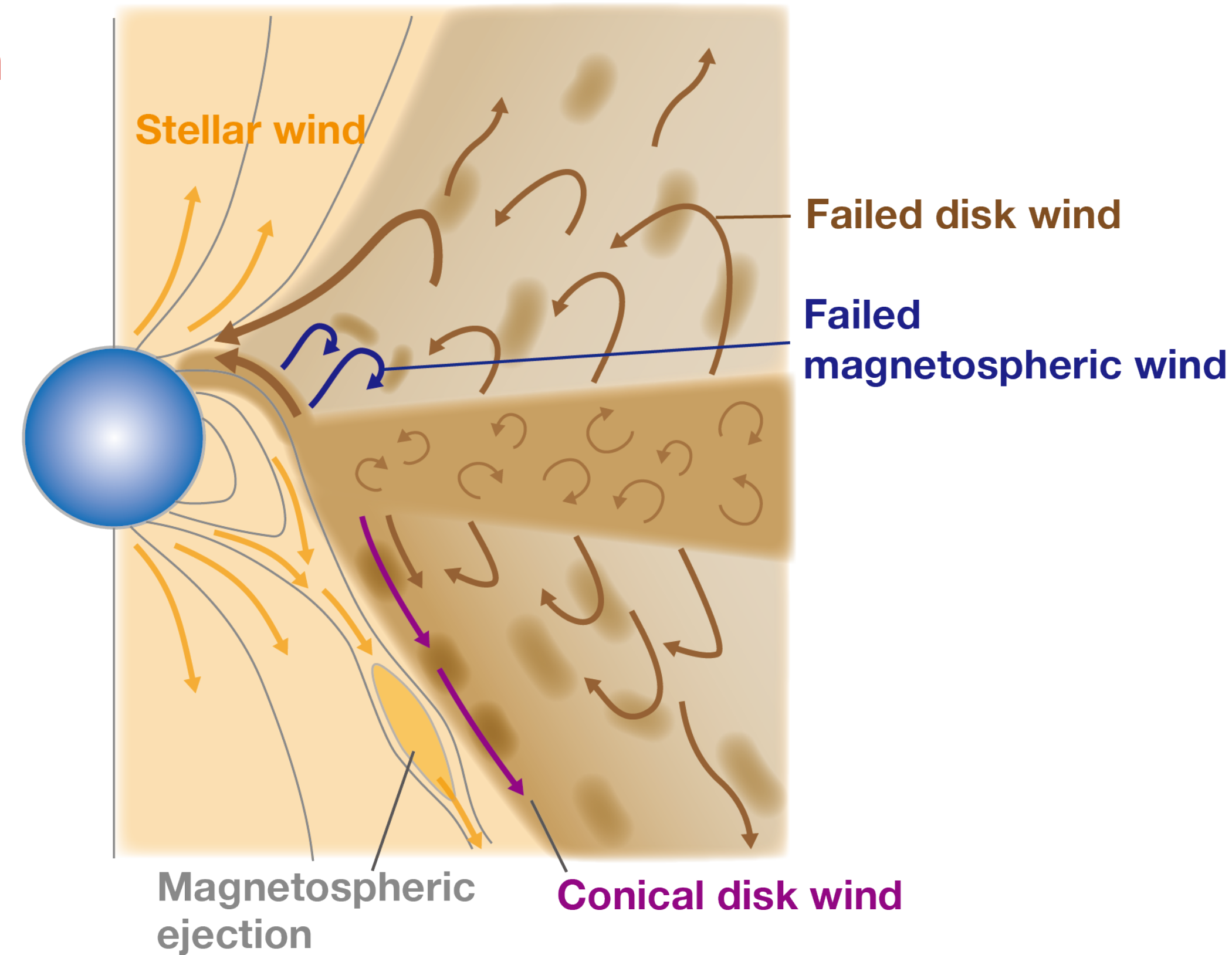


Magnetic spin-down torque

Accretion torque

Typical estimation of accretion torque

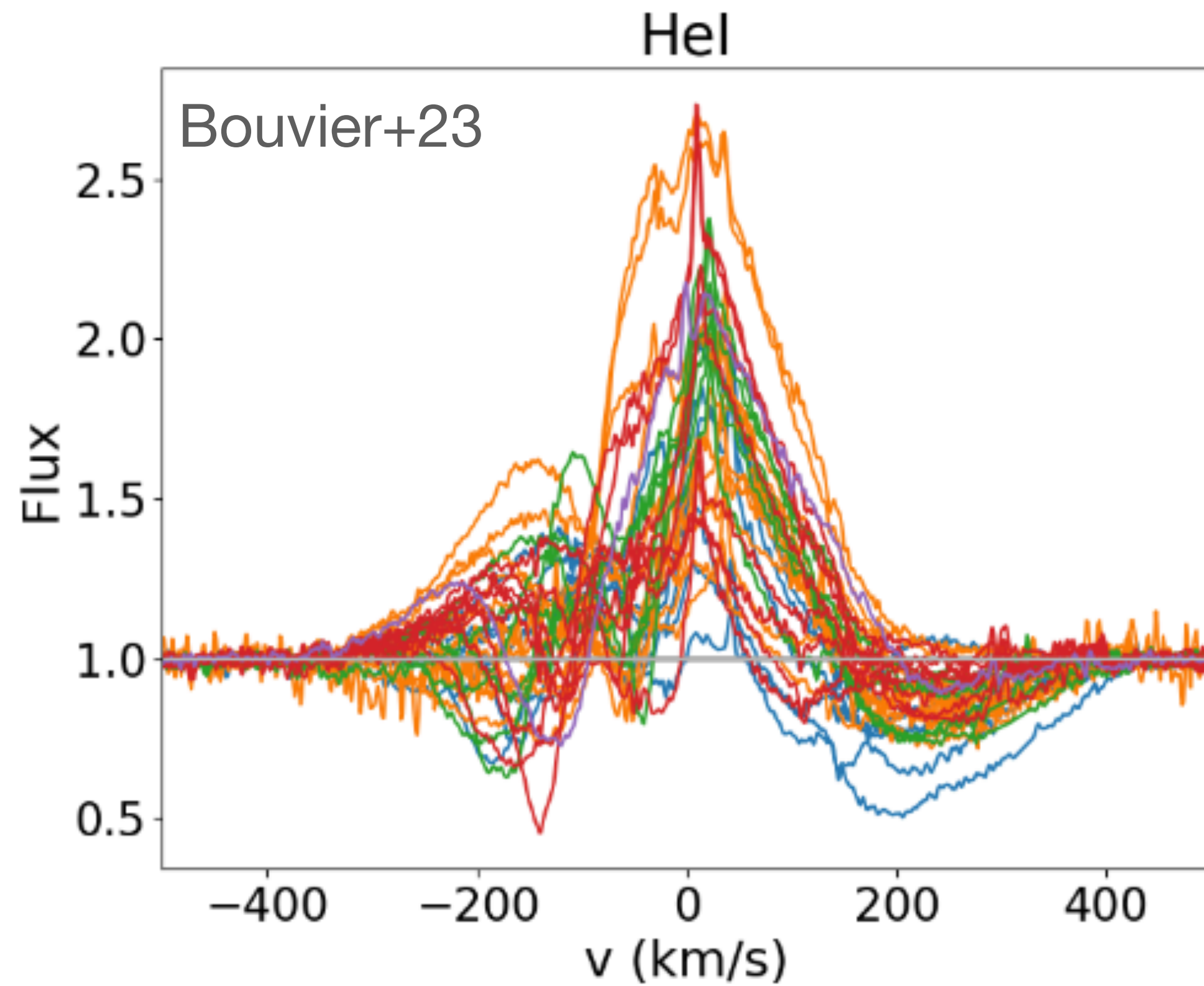
$$j' = \dot{M}_{\text{acc}} \sqrt{GM_* r_{\text{mag}}}$$



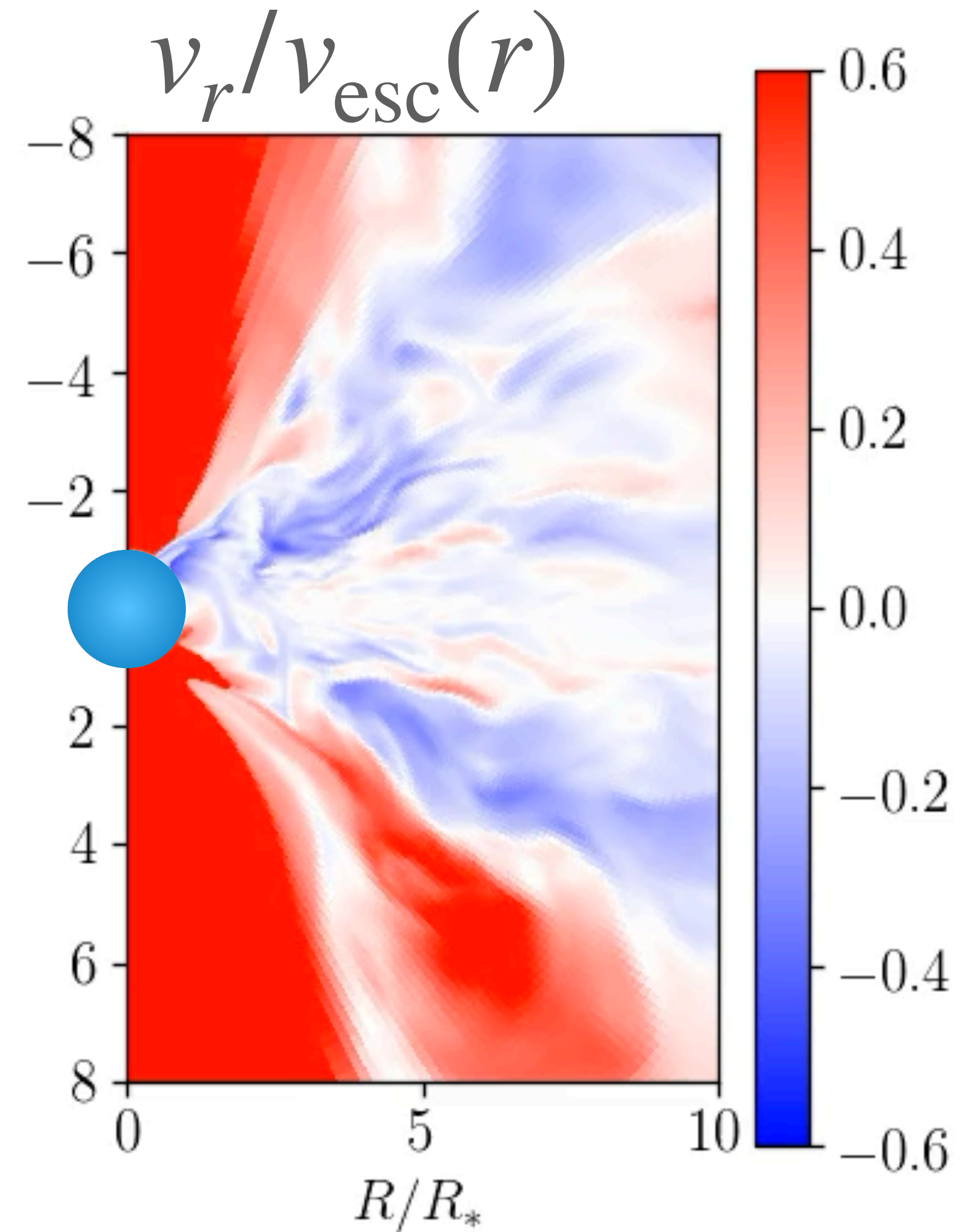
Slow, turbulent winds seem to extract angular momentum from accreting flows.
A possible key to solving the stellar spin-down problem.

Fluctuating atmosphere observed?

Variable red and blue components in He I line
(timescale \sim day)



An indication of mixture of accretion and outflow?

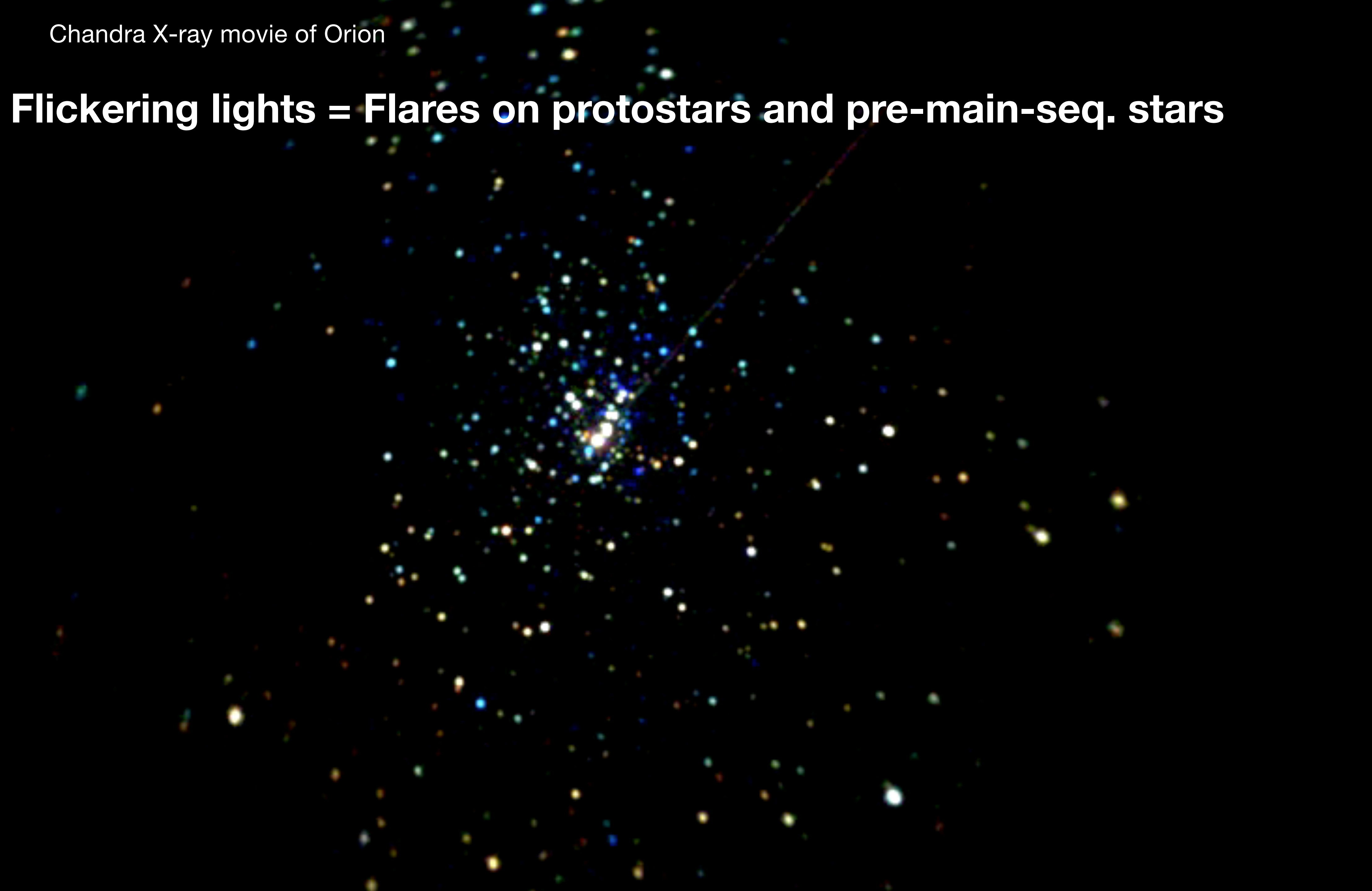


Explosive aspect of young stars



Chandra X-ray movie of Orion

Flickering lights = Flares on protostars and pre-main-seq. stars

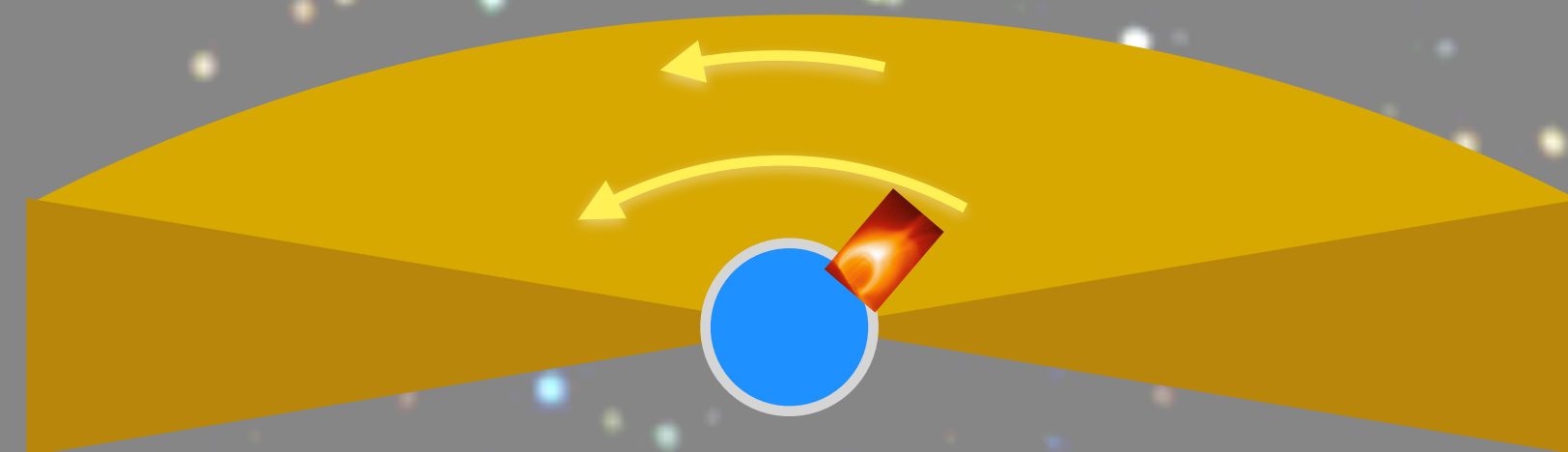


Flickering lights = Flares on protostars and pre-main-seq. stars

10^{34} - 10^{37} erg only in X-ray

>> flare energy of the largest solar flare ($\sim 10^{32}$ erg)

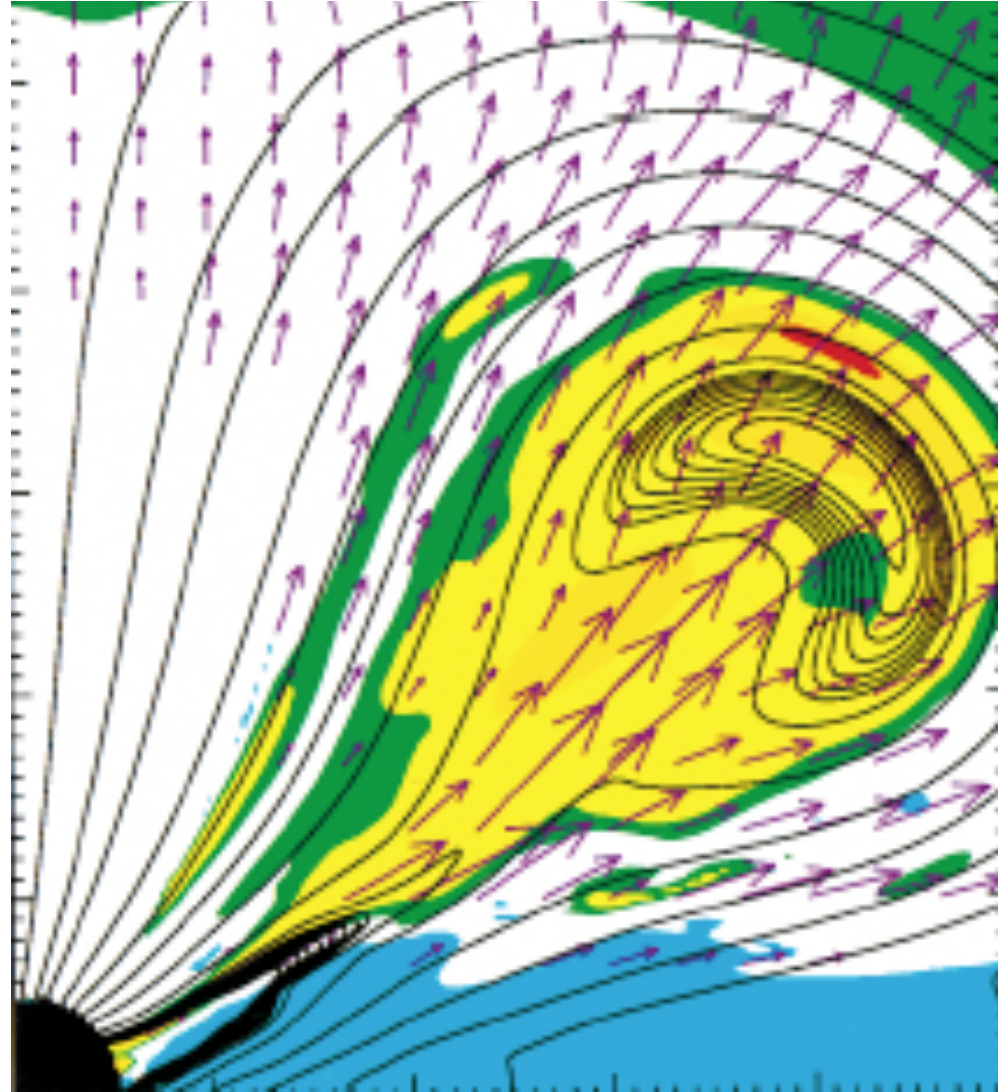
Disk



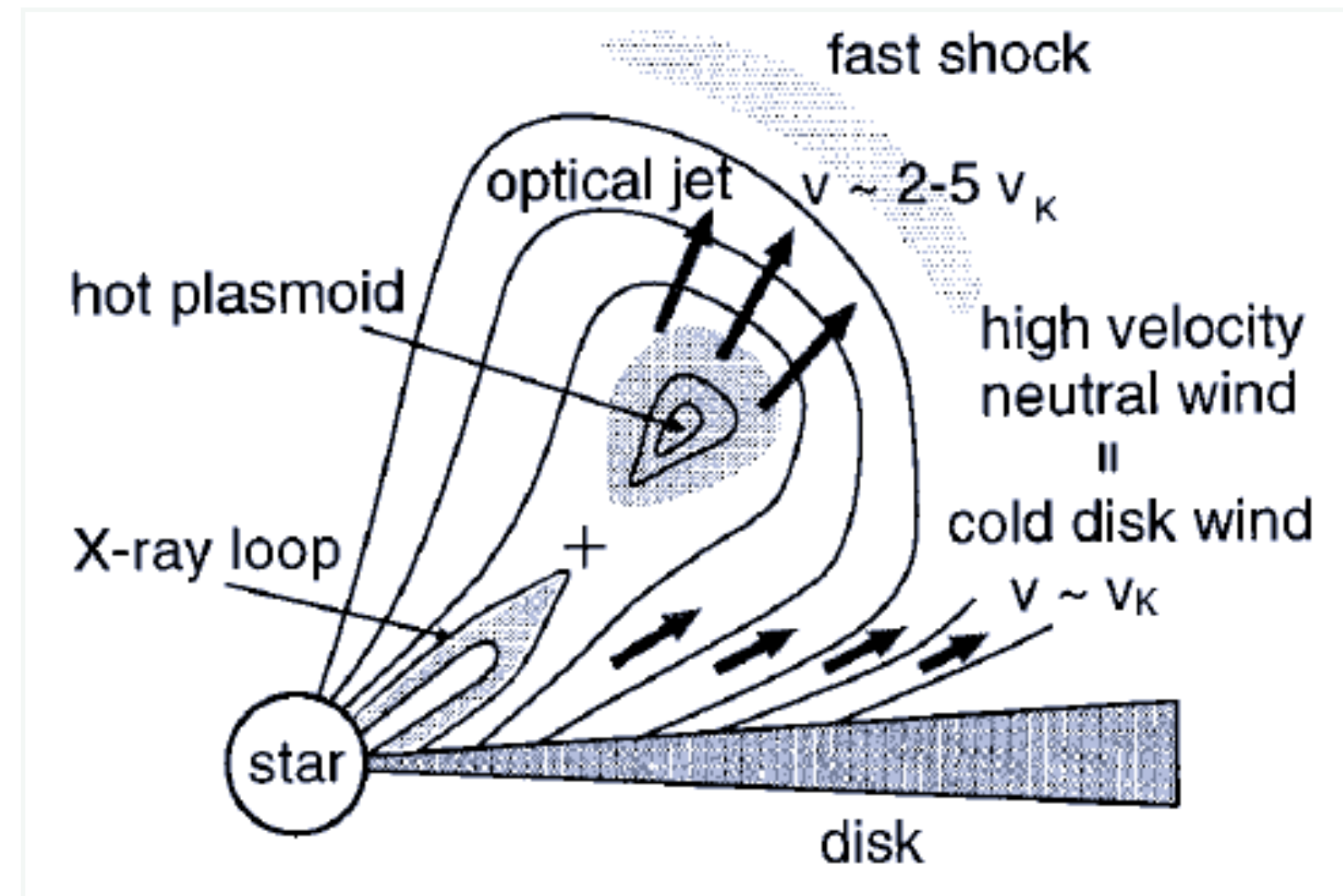
Mechanisms related to the accretion disk?

Magnetospheric ejection model

Hayashi+96



magnetospheric ejections



**Twisting the stellar field
by the rotating disk
(release of grav. energy)**

—> Eruption

See also, e.g., Shu+94, Hirose+97,
Zanni+13, Čemeljić+13, Ireland+20

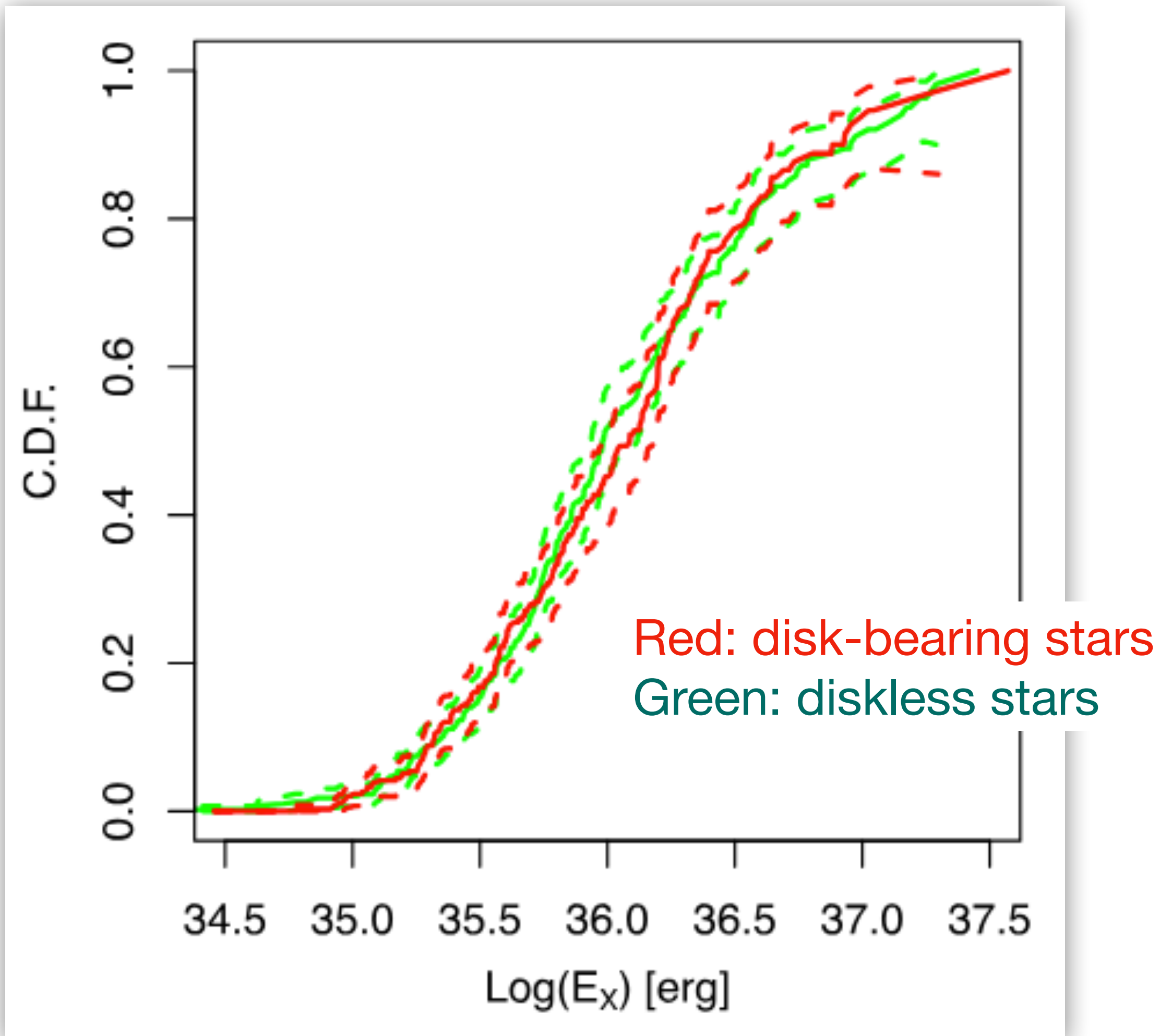
Predictions:

- High-accretors will produce stronger flares.
- Correlation between flare occurrence and stellar/disk rotation.
 - quasi-periodic production of flares
 - non-power-law flare occurrence rate

\Leftrightarrow power law for solar/stellar flares, $\text{Freq. [erg}^{-1}\text{yr}^{-1}] \propto E_{\text{flare}}^{-1.8}$ (Shibata+13)

Observations

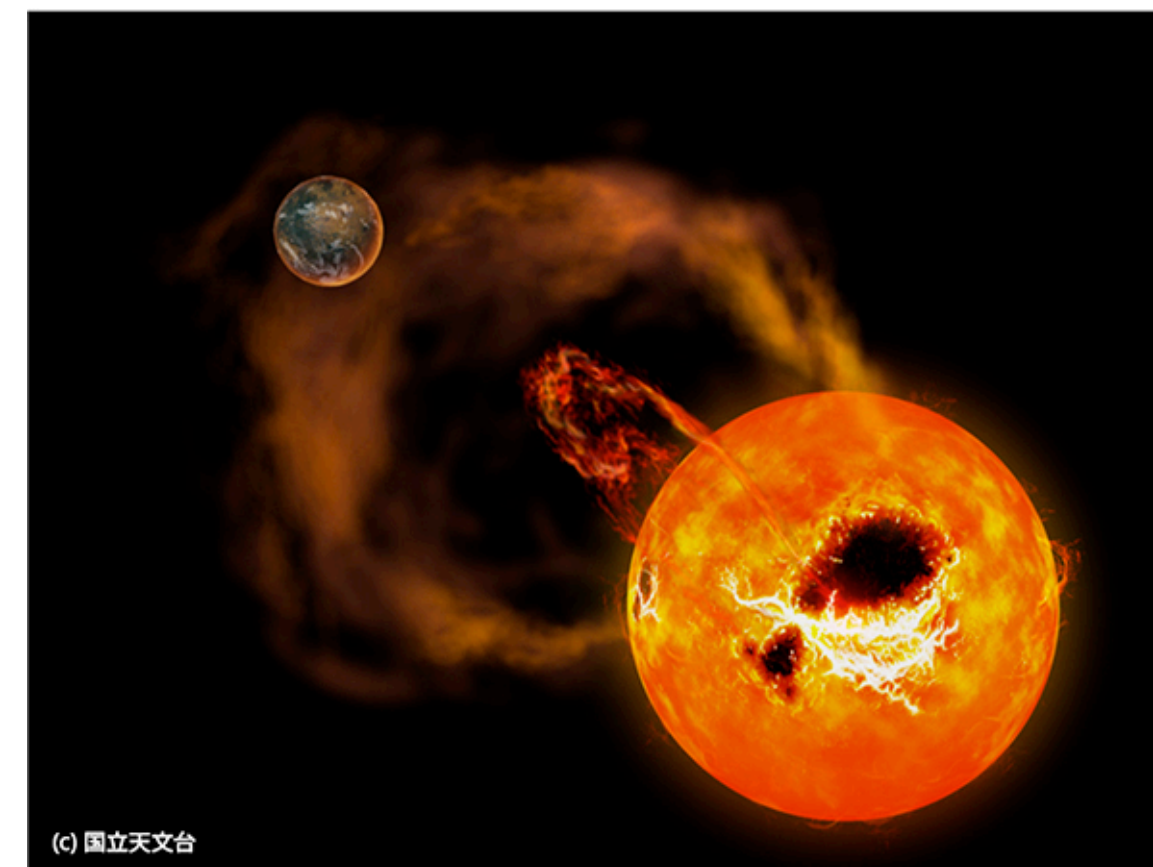
Getman & Feigelson 21



“no evidence for a distinct flaring mechanism involving the circumstellar disk”

See also Getman+08b

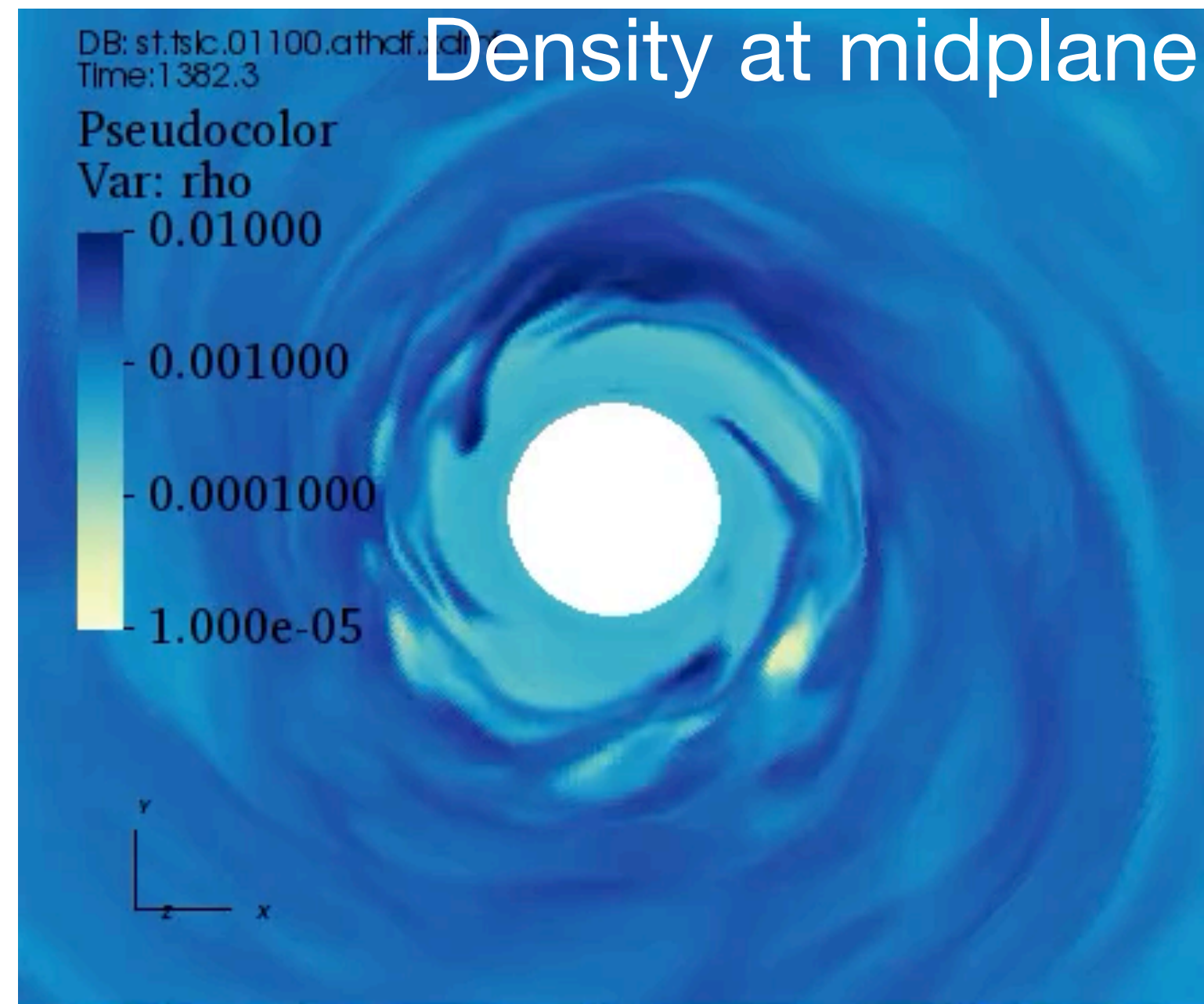
So flares on pre-MS stars should occur in the same way as MS stars.



Why star-disk interaction cannot produce huge flares efficiently?

3D effects on magnetospheric ejections

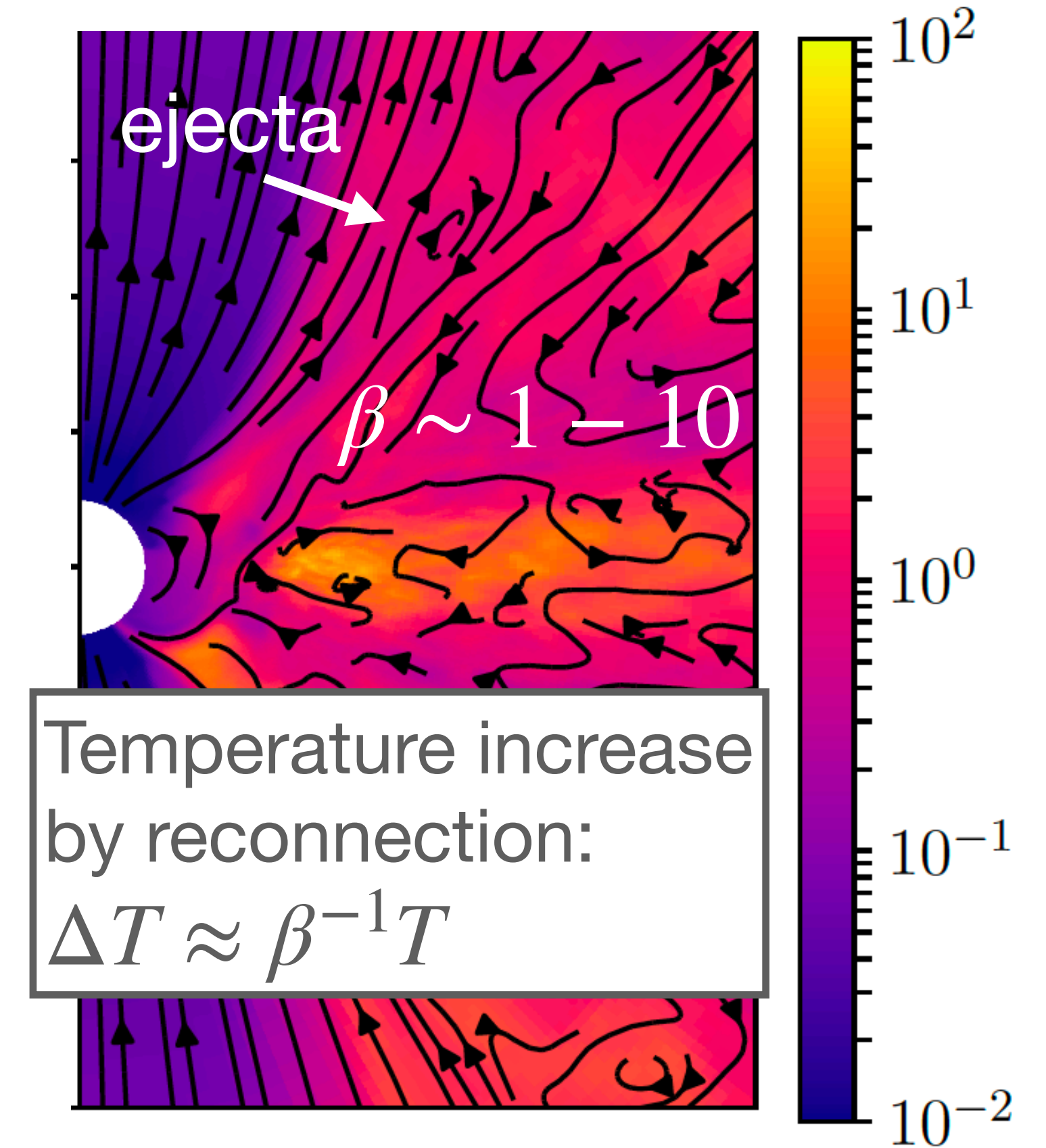
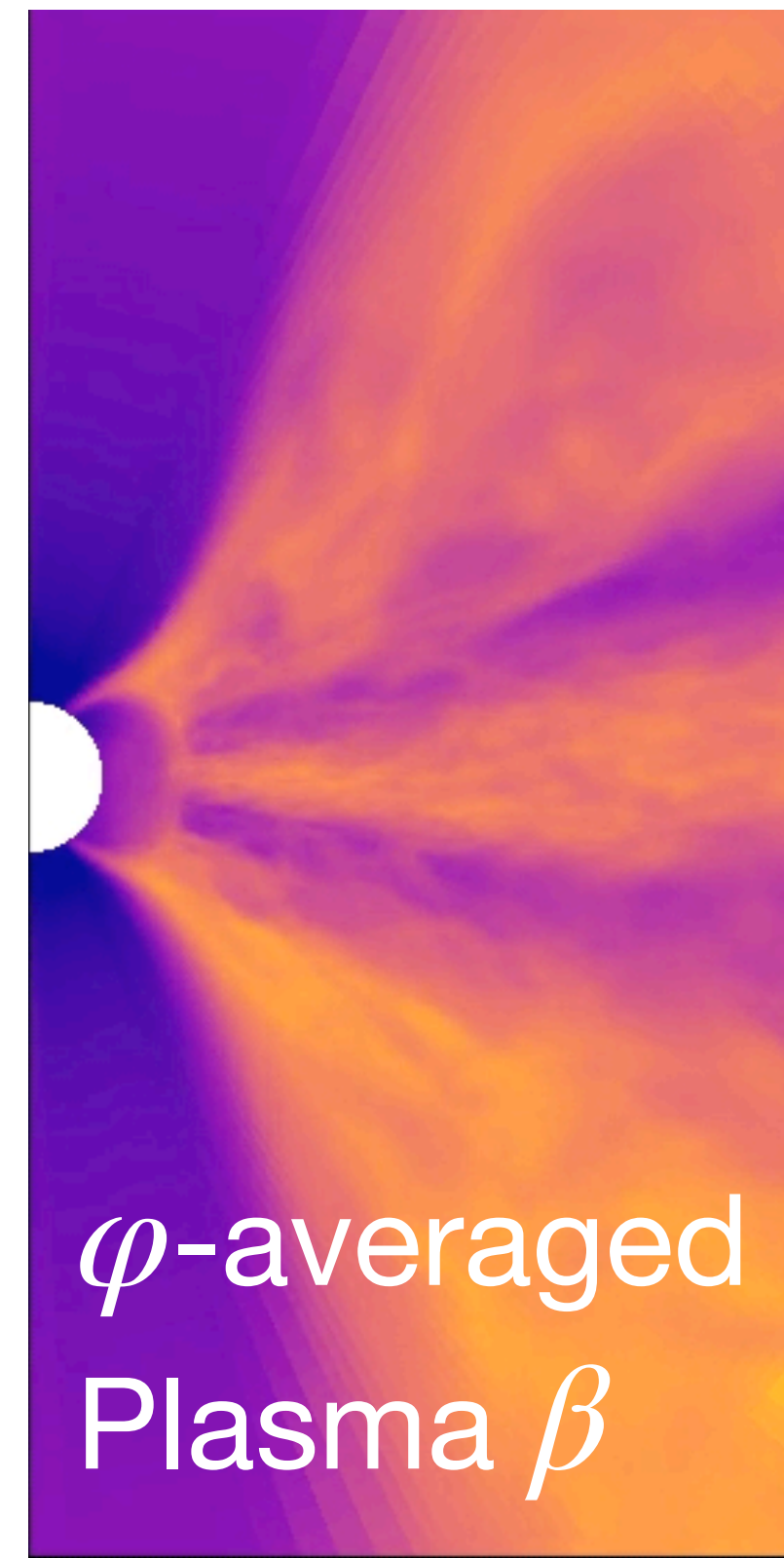
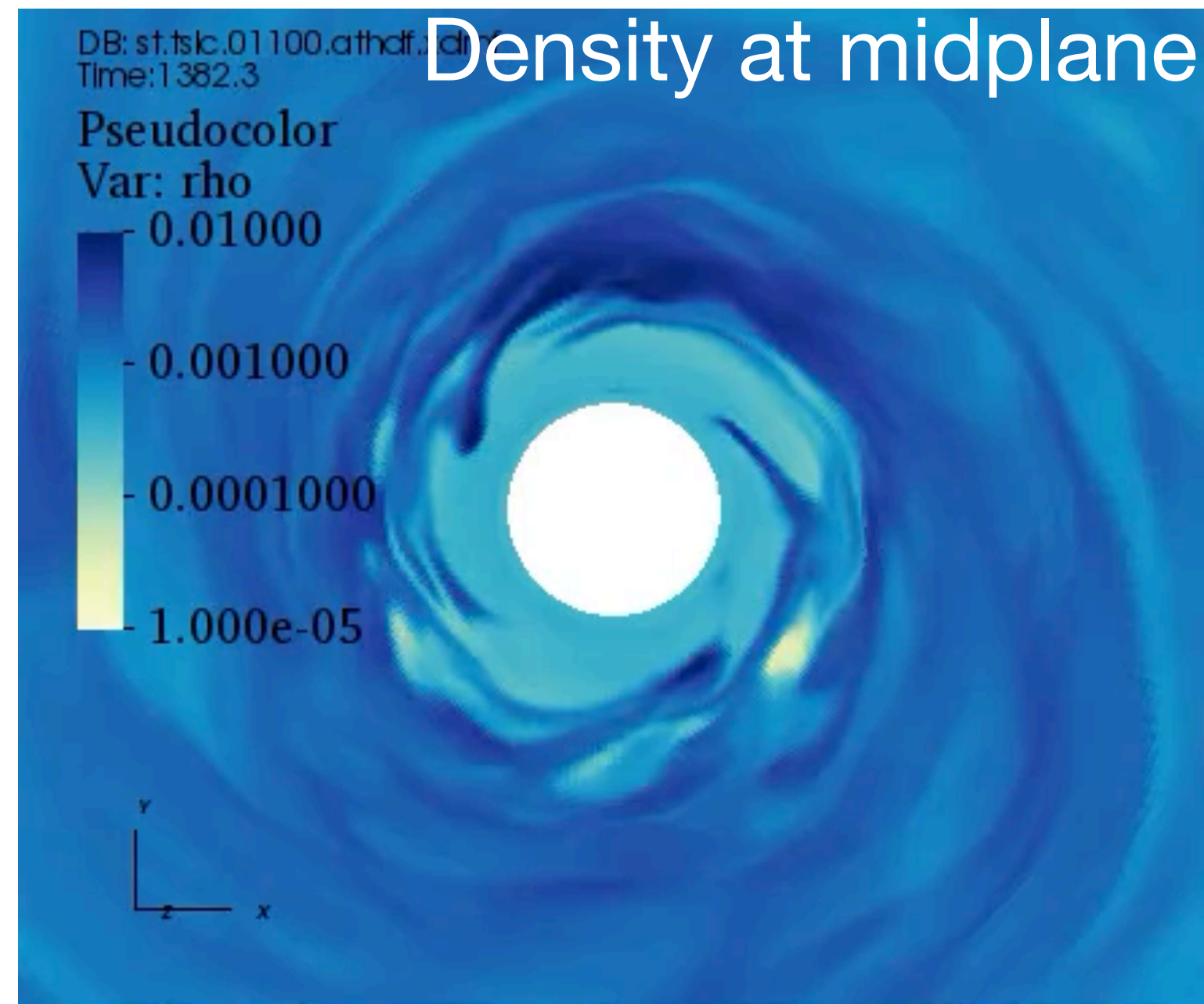
Eruptions occur in 3D models. But producing huge & hot flares is difficult!!



1. Fragmentation of accretion flow
—> inefficient twisting (energy build-up)

3D effects on magnetospheric ejections

Eruptions occur in 3D models. But producing huge & hot flares is difficult!!

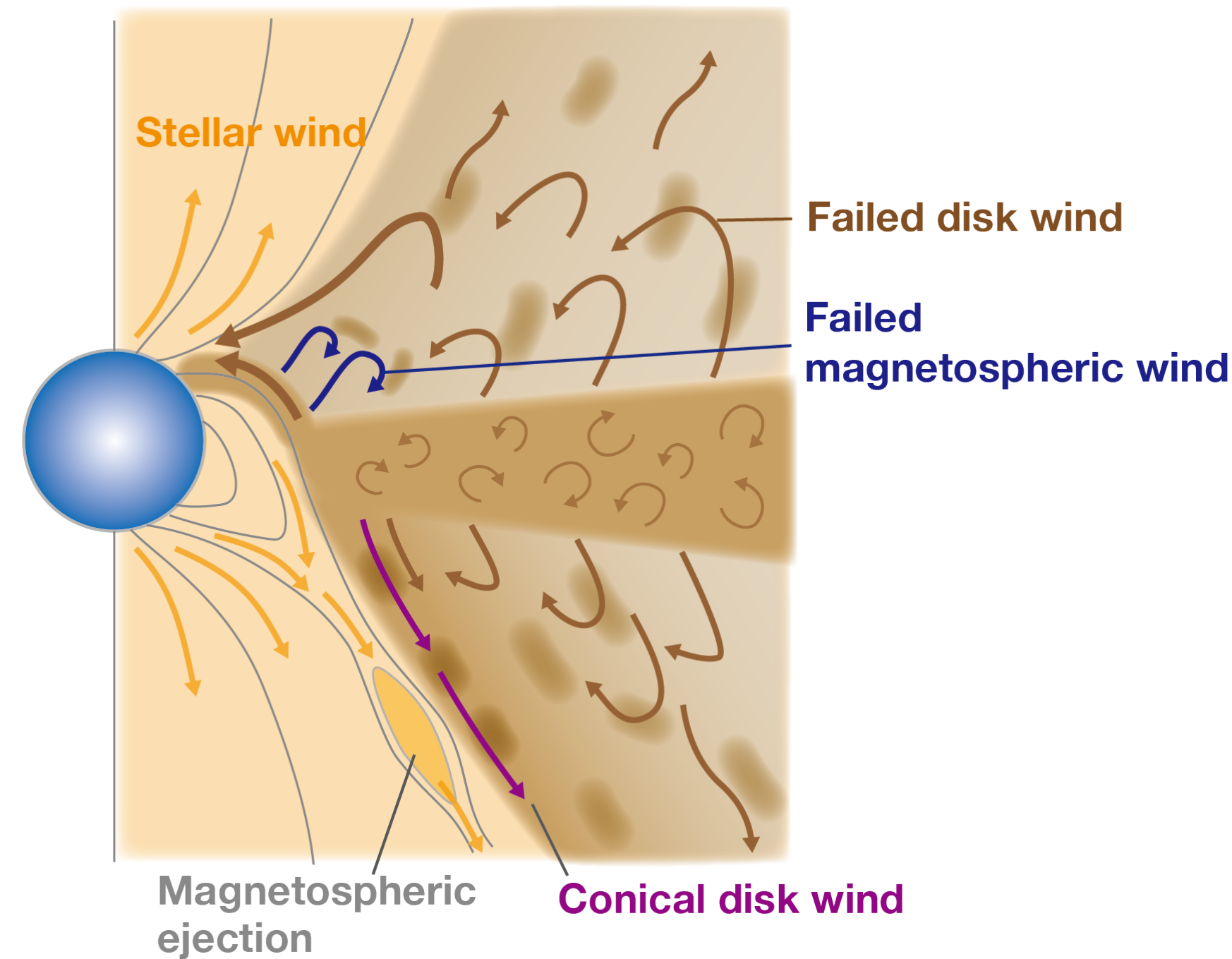
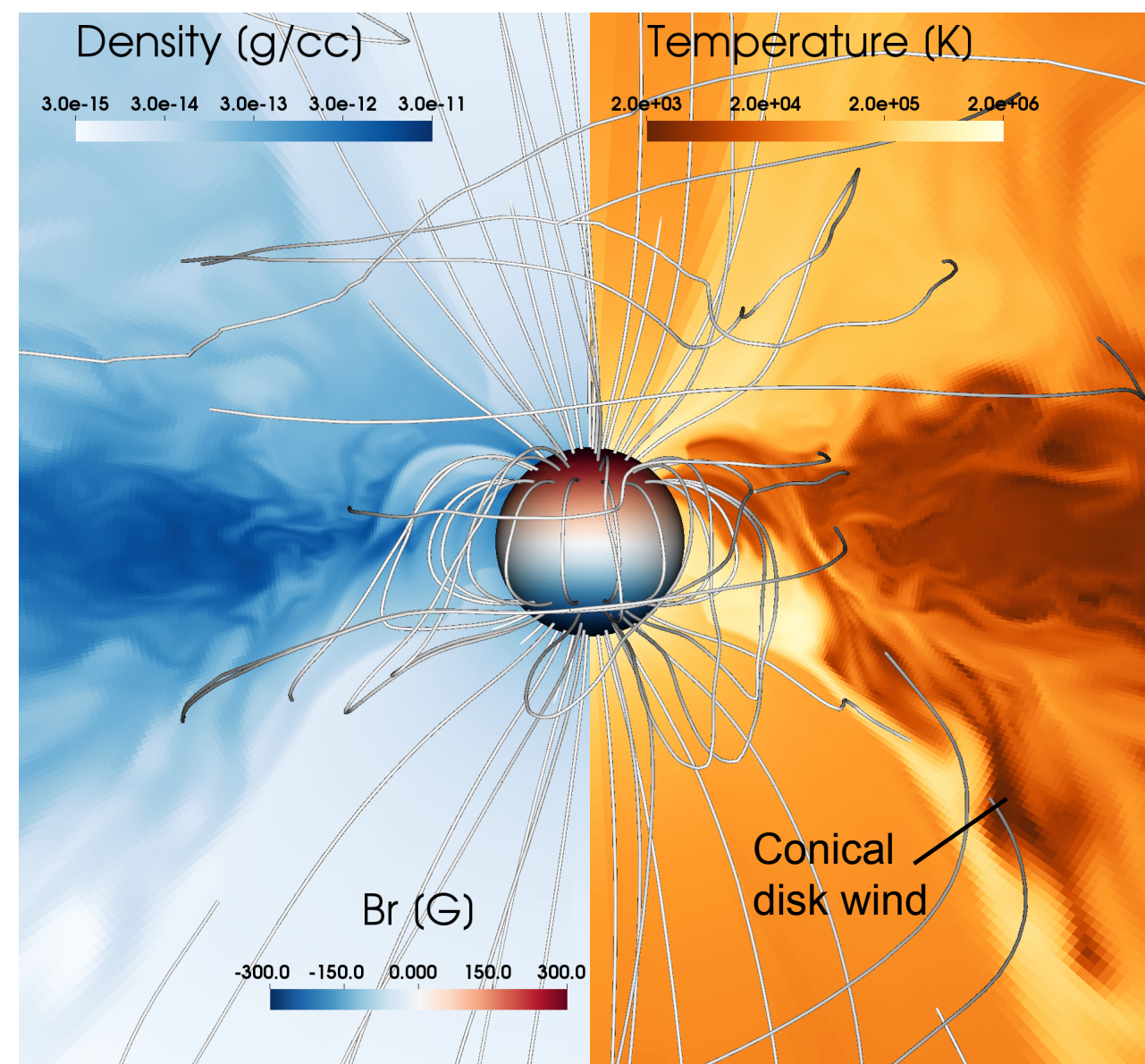


1. Fragmentation of accretion flow
—> inefficient twisting (energy build-up)

2. Reconnection cannot produce hot plasma
because of mass loading by the disk wind

Summary

We suggest an **updated picture of magnetospheric accretion** based on our 3D MHD simulations (Takasao et al. 2022)



Impacts of 3D effects:

- determination of magnetospheric radius
- origin of polar accretion flows (classical MA + failed disk wind)
- Suppression of spin-up torque
- Possible source of time variable line profiles
- Suppression of flaring activities driven by star-disk interaction